Nagra
Nationale
Genossenschaft
für die Lagerung
radioaktiver Abfälle

Cédra
Société coopérative
nationale
pour l'entreposage
de déchets radioactifs

Cisra
Società cooperativa
nazionale
per l'immagazzinamento
di scorie radioattive

TECHNICAL REPORT 91-11

THE ADSORPTION OF Cs^{+}, Sr^{2+} AND Ni^{2+} ON BITUMEN: A MECHANISTIC MODEL

L.R. VAN LOON,
Z. KOPAJTIC

JANUARY 1991

PSI, Würenlingen and Villigen

Parkstrasse 23 5401 Baden/Schweiz Telephon 056/20 55 11

Nagra
Nationale
Genossenschaft
für die Lagerung
radioaktiver Abfälle

Cédra
Société coopérative
nationale
pour l'entreposage
de déchets radioactifs

Cisra
Società cooperativa
nazionale
per l'immagazzinamento
di scorie radioattive

TECHNICAL REPORT 91-11

THE ADSORPTION OF Cs^{+}, Sr^{2+} AND Ni^{2+} ON BITUMEN: A MECHANISTIC MODEL

L.R. VAN LOON,
Z. KOPAJTIC

JANUARY 1991

PSI, Würenlingen and Villigen

Parkstrasse 23 5401 Baden/Schweiz Telephon 056/20 55 11

This report was prepared as an account of work sponsored by Nagra. The viewpoints presented and conclusions reached are those of the author(s) and do not necessarily represent those of Nagra.

Preface

In the framework of its Waste Management Programme, the Paul Scherrer Institute is performing work to increase the understanding of the geochemistry of nuclear waste relevant nuclides and the behaviour of solidification matrices. These investigations are performed in close cooperation with, and with the financial support of NAGRA. The present report is issued simultaneously as a PSI report and a NAGRA NTB.

Contents

Abstract

The adsorption of radionuclides on the waste matrix (cement, bitumen) is a positive effect and contributes to the retardation of released radionuclides migrating to the geo- and biosphere. For the safety assessment studies, it is important to know whether or not radionuclides do adsorb on the waste matrix.

In the present work, the adsorption of $^{134}Cs^{+}$, $^{85}Sr^{2+}$ and $^{63}Ni^{2+}$ on bitumen was studied as a function of the pH and ionic strength of the equilibrium solution. Bitumen emulsions with well defined surfaces were used.

The surface of bitumen is negatively charged due to the deprotonation of weak acid carboxyl groups at the interface. The functional group density amounts to $1.37 \cdot 10^{18}$ groups/m^2 and their deprotonation behaviour can be well described by the "Ionizable Surface Group" model.

Cs^{+}, Sr^{2+} and Ni^{2+} adsorb on the surface by three different processes, i.e. ion exchange, outer sphere complexation and inner sphere surface complexation respectively. The adsorption depends on the pH and the ionic strength of the contact solution. Under near field conditions (cementitious environment), Cs^{+} and Sr^{2+} do not adsorb on the bitumen due to the competition with Na^{+}, K^{+} and Ca^{2+} present in the cement pore water in contact with the bitumen.

Ni^{2+} adsorption can also be neglected because the formation of neutral and anionic hydroxo complexes in solution competes strongly with the adsorption reaction. Other hydrolysable radionuclides of interest are expected to behave similarly to Ni^{2+}.

The main conclusion of the study is that the adsorption of radionuclides (cations and anions) under near field conditions is expected to be very low (R_a : $10^{-4} - < 10^{-6}$ cm). Consequently, this process need not to be considered in safety assessment studies.

Résumé

L'adsorption des radionuclides sur la matrice des déchets (ciment, bitume) aurait un effet positif et contribuerait à retarder la migration des radionuclides relâchés vers la géosphère et la biosphère. Pour les modèles d'analyse de sécurité, il est important de savoir si les radionuclides sorbent à la matrice.

Dans le présent travail, la sorption du $^{137}Cs^{+}$, $^{85}Sr^{2+}$ et $^{63}Ni^{2+}$ sur le bitume pur a été étudiée en fonction du pH et de la force ionique de la solution d'équilibre. Des émulsions de bitume bien characterisées ont été utilisées.

La surface de bitume a une charge négative à cause de la déprotonation des groupes carboxyliques légèrement acides dans l'interface. La densité des groupes fonctionels atteint $1.37 \cdot 10^{18}$ groupes/m^2 et le modèle : "Ionisable Surface Group" décrit bien le comportement de la déprotonation.

Le Cs^{+}, le Sr^{2+} et le Ni^{2+} sorbent à la surface de bitume à la suite de trois processus differentes, à savoir : l'échange ionique, la complexation en sphère externe et la complexation en sphère interne. L'adsorption dépend du pH et la force ionique de la solution.

Dans les conditions du champ proche d'un dépôt de déchets radioactifs, Cs^{+} et Sr^{2+} ne sorbent pas sur le bitume à cause des compétitions avec Na^{+}, K^{+} et Ca^{2+} présents dans la solution dans les pores du ciment en contact avec le bitume.

La sorption de Ni^{2+} est aussi négligeable parce que la formation des complexes hydroxyliques neutres où négatifs dans la solution sont en compétition avec la sorption. On présume que d'autres radionuclides hydrolysables importants ont un comportement analogue à celui du Ni^{2+}.

La conclusion principale de cette étude est que l'adsorption des radionuclides (cations et anions) dans des conditions du champ proche d'un dépôt cimenté est très faible. Par conséquent, il n'y a aucun intérêt à considérer ce processus dans les études d'analyse de sécurité.

Zusammenfassung

Die Adsorption von Radionukliden an der Abfallmatrix (Zement, Bitumen) ist ein positiver Effekt und trägt zur Verlangsamung der Nuklidwanderung zur Geo- und Biosphäre bei. In Bezug auf die Sicherheitsanalyse ist es wichtig zu wissen, ob die Nuklide an der Abfallmatrix adsorbieren oder nicht.

In der vorliegenden Arbeit wurde die Adsorption von $^{134}Cs^{+}$, $^{85}Sr^{2+}$ und $^{63}Ni^{2+}$ an Bitumen als Funktion des pH-Werts und der Ionenstärke der Gleichgewichtslösung untersucht. Es wurden Bitumen-in-Wasser Emulsionen mit gut definierten Oberflächen benutzt.

Die Bitumen/Wasser Grenzfläche ist, aufgrund der Deprotonierung von Carboxylgruppen an der Oberfläche, negativ geladen. Die Dichte der funktionellen Gruppen beträgt $1.37 \cdot 10^{18}$ Gruppen/m^2 und ihr Deprotonierungsverhalten kann gut mit dem "Ionizable Surface Group" –Modell beschrieben werden.

Cs^{+}, Sr^{2+} und Ni^{2+} adsorbieren an der Oberfläche nach drei verschiedenen Prozessen, d.h. Ionenaustausch und durch Bildung von ausser-bzw. innersphärischen Oberflächenkomplexen. Die Adsorption hängt vom pH-Wert und von der Ionenstärke der Lösung ab. Unter Nahfeldbedingungen adsorbieren Cs^{+} und Sr^{2+} am Bitumen aufgrund der Konkurrenz mit Na^{+}, K^{+} und Ca^{2+}–Ionen, welche im Zementporenwasser vorhanden sind, nicht.

Eine Ni^{2+}–Adsorption kan ebenfalls vernachlässigt werden, weil die Bildung von neutralen und anionischen Hydroxokomplexen in der Lösung die Adsorptionsreaktion stark konkurrenziert. Es wird erwartet, dass andere hydrolysierbare Radionuklide von Bedeutung ein ähnliches Verhalten aufweisen wie Ni^{2+}.

Die Hauptschlussfolgerung dieser Studie führt zur Aussage, dass unter Nahfeldbedingungen lediglich ein sehr schwache Adsorption von Radionukliden (Kationen und Anionen) erwartet wird (R_a : 10^{-4} – < 10^{-6} cm). Infolgedessen ist es wenig sinnvoll, die Adsorption von Radionukliden an Bitumen in der Sicherheitsanalyse zu berücksichtigen.

1 Introduction

The suitability of a material to be used as solidifying matrix for radioactive wastes is determined by many factors, including:

- High resistance of the material to leaching of radionuclides by water
- Resistance to damage from irradiation
- Good adsorption characteristics for radionuclides

For bitumen, the first two characteristics are acceptable, as long as the activity contained does not exceed 1 Ci/L. The maximum admissible activity to be embedded is thereby limited more by gas release than by leach rate [13].

Only a small amount of reliable information on the adsorption of radionuclides on bitumen is available.
Burnay [5] studied the adsorption of ^{137}Cs on crushed bitumen in demineralized water. Adsorption was expressed as K_d on a mass basis (m^3/kg). The adsorption was time dependent and increased after irradiation of the bitumen. No mechanistic processes were studied or even considered in his work.

Hietanen et al. [14] studied the adsorption of ^{134}Cs, ^{85}Sr, ^{63}Ni, ^{14}C and ^{125}I on crushed bitumen in a groundwater medium. They found adsorption of all radionuclides. The K_d values (cm^3/g) decreased for decreasing volume/mass ratios.
Alaluusua and Hakanen [1] also studied the adsorption of ^{134}Cs, ^{85}Sr, ^{60}Co and ^{99}Tc on bitumen in groundwater equilibrated with concrete. They also found adsorption for all radionuclides. In general, adsorption increased with time. It is of course questionable whether elements as C, I and Tc have really been adsorbed on the negatively charged bitumen, because these three elements are present as anions.

A common disadvantage of the three studies was the use of undefined bitumen surfaces in their experiments and the expression of adsorption (K_d) on a mass basis. The total surface to which radionuclides are exposed and not the mass is relevant for adsorption. Therefore, the expression of K_d on a mass basis (cm^3/g) is, in fact, useless for safety assessment studies unless a good conversion factor (cm^2/g) is available. Further, no information is available on effects of ionic strength, pH and composition of the equilibrium water and, more importantly, mechanistic insight is lacking.

The present work describes the adsorption of $^{134}Cs^+$, $^{85}Sr^{2+}$ and $^{63}Ni^{2+}$ on a pure bitumen (Mexphalt 80/100). Bitumen emulsions with well defined surfaces were used instead of crushed bitumen. This allowed us to collect reliable information on the adsorption of these nuclides and to express the adsorption on a surface area basis (cm). Effects of ionic strength and pH were studied and the results could be explained satisfactorily by an ion exchange/surface complexation model combined with the Ionizable Surface Groups model [6,26]. On the basis of these results, the potential adsorption of radionuclides on bitumen in a cementituous environment could be evaluated.

2 The electric properties of the bitumen/water interface

The knowledge on the electric properties of bitumen/water interfaces has increased ever since the basis of the hot water process for recovering bitumen and oil from tar sands was understood [25,27,28]. The hot water process induces a separation between bitumen and mineral phases by mixing the oil sand in a conditioning drum with hot water and a process aid, usually sodium hydroxide. The amount of NaOH is the major variable used to optimize the process or to maximize the recovery of the oil or bitumen.
The basis for the process is the fact that both the bitumen and sand surfaces are negatively charged at high pH values, resulting in repulsion between these particles. The process, however, is influenced by the Na^+ and K^+ concentration and the presence of Ca^{2+}. The presence of Ca^{2+} causes a drastic decrease in the effect of NaOH on bitumen recovery [28].

Bitumen has a rather complicated composition. Important for the electric properties of the bitumen/water interface is the presence of polar organic components with surface active characteristics (natural surfactants).
The most important anion-active compounds present in bitumen are [19]:

– naphtenic acid

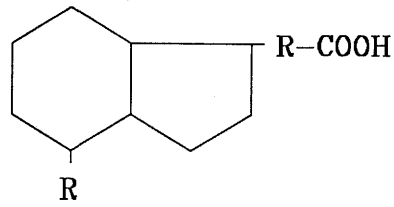

– naphtenic-aromatic acids

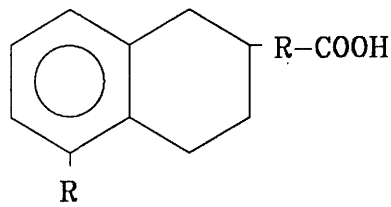

The carboxyl groups are not bound on the rings, but on an alkyl chain [19]. The natural polar substances in bitumen are able to stabilize bitumen–in–water emulsions. To stabilize these emulsions, the water phase must be made alkaline.
The surface charge of the bitumen is thus caused by the dissociation of carboxyl groups at the bitumen/water interface. The electric properties of the interface can be explained by the Ionizable Surface-Group Model [6,26]. A brief description of the model is given here.

Assume the following deprotonation reaction of a carboxyl group on a surface:

$$RCOOH \rightleftharpoons RCOO^- + H^+ \tag{1}$$

The deprotonation constant is given by:

$$K_H = \frac{\{RCOO^-\} \cdot [H^+]_s}{\{RCOOH\}} \tag{2}$$

where $[H^+]_s$ is the concentration of hydrogen ions close to the surface, given in mol/L. The concentration of protonated and deprotonated groups is expressed as groups/cm^2. The concentration of H^+ on the surface $[H^+]_s$ is related to the bulk H^+ concentration $[H^+]_b$ by the Boltzmann equation:

$$\left[H^+\right]_s = \left[H^+\right]_b \, exp(-Y_o) \tag{3}$$

where Y_o is the reduced surface potential, defined as $Y_o = \frac{e\psi_o}{kT}$

with : e = the elementary charge ($1.6 \cdot 10^{-19}$ C)
ψ_o = the surface potential (V)
k = the Boltzmann constant ($1.38 \cdot 10^{-23}$ J K^{-1})
T = the absolute temperature (K)

As the potential ψ_o is negative for bitumen, the term $exp(-Y_o) > 1$, and this implies that the hydrogen ion concentration on the surface is higher than the hydrogen ion concentration of the bulk solution, or the surface pH is lower than the solution pH. This phenomenon has already been observed and described earlier by Danielli [9]. The difference in pH between surface and bulk solution can amount to several pH units. For instance, when the surface potential ψ_o equals –200 mV, the pH of the surface is 4 pH units lower than the pH of the bulk solution [24]. Weak acid functional groups at interfaces display an apparent acid character ascribable to, and determined in magnitude by, the electrical potential ψ_o generated upon ionization of the interface. As a result, the dissociation of the surface weak acid groups will only be complete at higher pH values in solution than would be the case for a monomeric weak acid in solution.

The surface charge of the bitumen is caused by the dissociated carboxyl groups and is given by:

$$\sigma_o = -e \cdot \{RCOO^-\} \tag{4}$$

The total surface density of functional groups (N_s, groups/cm^2) is given by :

$$N_s = \{RCOO^-\} + \{RCOOH\} \tag{5}$$

The surface charge (σ_o, C/cm^2) can thus be written as :

$$\sigma_o = \frac{-eN_s}{1 + ([H^+]_b/K_H)exp(-Y_o)} \tag{6}$$

The surface charge has to be neutralized by the charge in the diffuse electrical double layer (σ_d) :

$$\sigma_o = -\sigma_d \tag{7}$$

The charge density in the diffuse double layer can be related to the surface potential by applying the Gouy-Chapman theory :

$$\sigma_d = -(8n\varepsilon kT)^{1/2} \; sinh \; (zY_o/2) \tag{8}$$

with : n = number of counter ions per unit volume (cm^{-3})
z = valency of the counter ions
ε = permittivity of the medium (C V^{-1} cm^{-1})

Combination of equations (6) and (8) provides an explicit relationship between surface charge and surface potential as a function of pH$_b$, the salt concentration and the density of functional groups N_s on the surface :

$$pH_b = -Y_o/2.303 + pK_H - log\left(\frac{\theta}{sinh(zY_o/2)} - 1\right) \tag{9}$$

where $\theta = \frac{-eN_s}{(8n\varepsilon kT)^{1/2}}$

This relationship enables one to calculate the surface potential at a given pH_b, ionic strength and amount of functional groups. The corresponding σ_o can be calculated by applying equation (8), assuming that $\sigma_o = -\sigma_d$. Figure 2.1 displays the relationship between the level of dissociation α and the bulk pH_b as a function of the salt concentration in the solution and functional group density on the surface. It is clear that the deprotonation behaviour of the carboxyl groups is complex and depends strongly on the surface group density and ionic strength of the medium.

3 Preparation and characterization of bitumen emulsions

3.1 Materials and methods

3.1.1 Preparation of bitumen – in – water emulsions

About 10 g of bitumen (Mexphalt 80/100) were placed in a 500 ml flask. Approximately 400 ml of a 10^{-3} M NaOH (pH = 11) were added, the mixture heated to 80 - 90 °C and then stirred vigorously at 24000 rpm for 5 minutes by a high speed mixer (Ultra-Turrax, T-25; Janke & Kunkel, IKA). After cooling, the emulsion was pored into an Erlenmeyer flask and left standing overnight.
Two 50 ml aliquots of the emulsion were placed in dialysis bags (Dialysis Tubing-Visking, Medicell, London) and dialysed against 1L solution of the desired composition. The bags were shaken in an end–over–end shaker. The solution was replaced 4 times at intervals of about 2 hours. After the fourth replacement, the conditioned bitumen emulsion was filtered through a 40 μm nominal pore size nylon membrane (Nytal, nylon monofilament). The filtered solution was used for adsorption experiments, dry weight determination, particle size analysis and surface group density measurements.

3.1.2 Dry weight determination

10 ml of the bitumen emulsion were placed in a preweighed petri-dish and dried at 50°C for 24 hours. After correction for the presence of salts, the dry weight was calculated.

3.1.3 Particle size analysis

The particle size distribution of the emulsion was measured by a Coulter-Multisizer (Coulter Electronics Limited). The Coulter Counter determines the number and size of particles suspended in an electrically conducting liquid, by forcing the suspension through a small aperture having an immersed electrode on either side. As a particle passes through the aperture, the resistance between the electrodes changes and produces a voltage pulse whose magnitude is proportional to the particle size. Isoton (II) was used as the conducting fluid and an orifice tube of 50 μm was selected, which has a measurement range from 1 to 30 μm. The apparatus was calibrated by latex particles with a nominal diameter of 5.8 μm. Size distributions for particles smaller than 1 μm were determined with a laser diffraction particle size distribution analyzer (Horiba LA-500). This apparatus had a measuring range from 0.1 μm to 200 μm. The specific surface area (SSA) was calculated from the particle size distribution, assuming the bitumen particles to be spherical. The calculation was carried out by an automatic procedure available in the apparatus.

3.1.4 Surface group density determination

Different techniques for the determination of the surface group density are known. The most common one available for weak acid groups, acid/base titration, however, could not be applied for bitumen emulsions for several reasons. The most important reason

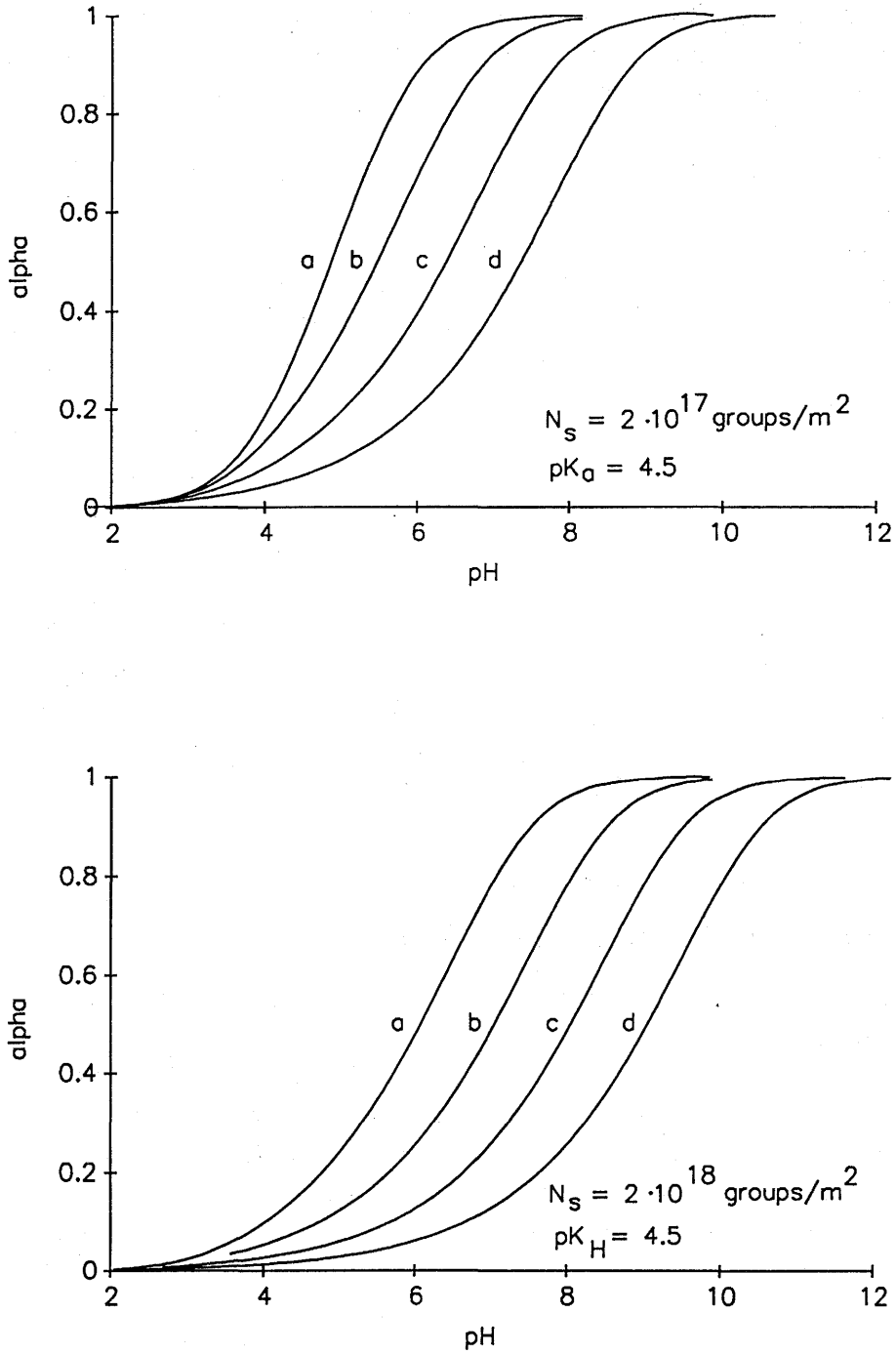

Figure 2.1: Dissociation of surface carboxyl groups as a function of pH and ionic strength for two surface group densities (N_s).
a) I=0.1 M; b) I=0.01 M; c) I=0.001 M; d) I=0.0001 M

was the low concentration of the functional groups in the emulsions (1-10 μmol/L).

We therefore selected a classical technique based on the adsorption of an index cation on the bitumen surface. $Co(NH_3)_6^{3+}$ was used as index cation. This technique has recently been used successfully to the determination of the functional group capacity of humic acids [16] and in previous studies to measure the cation exchange capacities of metal oxides [8], clay minerals [18] and polyacrylic acids [12].
$Co(NH_3)_6^{3+}$ is stable in aqueous solutions between pH 2 and 12. It adsorbs only due to Coulombic interaction and charge reversal due to over– equivalent adsorption is excluded [8]. The negative charge on the surface is almost completely neutralized by the electrostatically adsorbed $Co(NH_3)_6^{3+}$. One mol of adsorbed $Co(NH_3)_6^{3+}$ represents three moles of negative charges on the surface. $Co(NH_3)_6^{3+}$ can therefore be used very well to determine the total amount of functional groups on bitumen under conditions where they are completely dissociated (high pH).
An adsorption isotherm of $Co(NH_3)_6^{3+}$ on bitumen was performed. A bitumen emulsion was prepared as described in 3.1.1. 20 ml aliquots of the emulsion were placed in a teflon centrifuge tube (Oak Ridge Type, 50 ml) and different volumes of a 10^{-4} M $Co(NH_3)_6^{3+}$ solution were added. The volume in each centrifuge tube was then made up to 30 ml by 10^{-3} M NaOH. The mixtures were shaken end-over-end for 24 hours at room temperature. After equilibration, the solutions were centrifuged at 11000 g (Heraeus Sepatech, Biofuge 17S) for 30 minutes. The clear supernatant was analyzed for Co by ICP-AES. The amount of $Co(NH_3)_6^{3+}$ adsorbed was calculated from the difference in Co concentration before and after equilibrium. The plateau value of the isotherm was taken as the functional group density of the bitumen.

3.2 Results and discussion

3.2.1 Particle size distribution of bitumen droplets

Figure 3.1 shows an electron micrograph of the bitumen particles. The shape of the particles is spherical.
Figure 3.2 displays the particle size distribution of bitumen droplets in a 10^{-3} M NaOH solution. The particle diameter of the bitumen droplets varies from 0.1 to 15 μm. Measurements with the Coulter Counter thus gives incomplete distributions and, as a result, underestimations of the specific surface area (SSA). Table 3.1 gives an overview of the specific surface areas of two emulsions measured by the two different techniques. The Coulter-Counter gives a specific surface area of about 3 times lower than the Laser Diffraction particle size analyser. A better measurement with the Coulter Counter can be obtained by applying a smaller orifice tube. The lower limit, however, is still 0.4 μm. As measurements with smaller orifice tubes require prior treatment of the samples to remove particles larger than the upper limit and since this is a time consuming procedure, we preferred to correct the results obtained by the 50 μm orifice tube by a factor three in all later experiments (The laser diffraction technique was only available for a short period).

Table 3.1: Specific surface area of bitumen emulsions determined by two different techniques

Coulter Counter 50 μm orifice tube	Laser diffraction Horiba LA-500	Laser/Coulter
1.35 m^2/g	3.81 m^2/g	3.03
1.40 m^2/g	4.24 m^2/g	2.82
		2.92

Table 3.2: Overview of the concentration and the specific surface area (SSA) of different bitumen–in–water emulsions

Medium	Dry weight %	Specific surface area m^2/g
10^{-3} M NaOH	0.283	3.54
10^{-3} M NaOH	0.280	4.20
10^{-3} M NaOH	0.215	3.92
10^{-3} M NaOH + 10^{-3} M $NaClO_4$	0.239	4.38
10^{-3} M NaOH + 10^{-3} M $NaClO_4$	0.222	4.48
10^{-3} M NaOH + 10^{-3} M $NaClO_4$	0.284	3.73
10^{-3} M NaOH + $4 \cdot 10^{-3}$ M $NaClO_4$	0.298	3.71
10^{-3} M NaOH + $9 \cdot 10^{-3}$ M $NaClO_4$	0.307	3.72
10^{-3} M NaOH + $0.5 \cdot 10^{-3}$ M $NaClO_4$	0.221	4.22
10^{-3} M NaOH + $9 \cdot 10^{-3}$ M $NaClO_4$	0.205	3.76

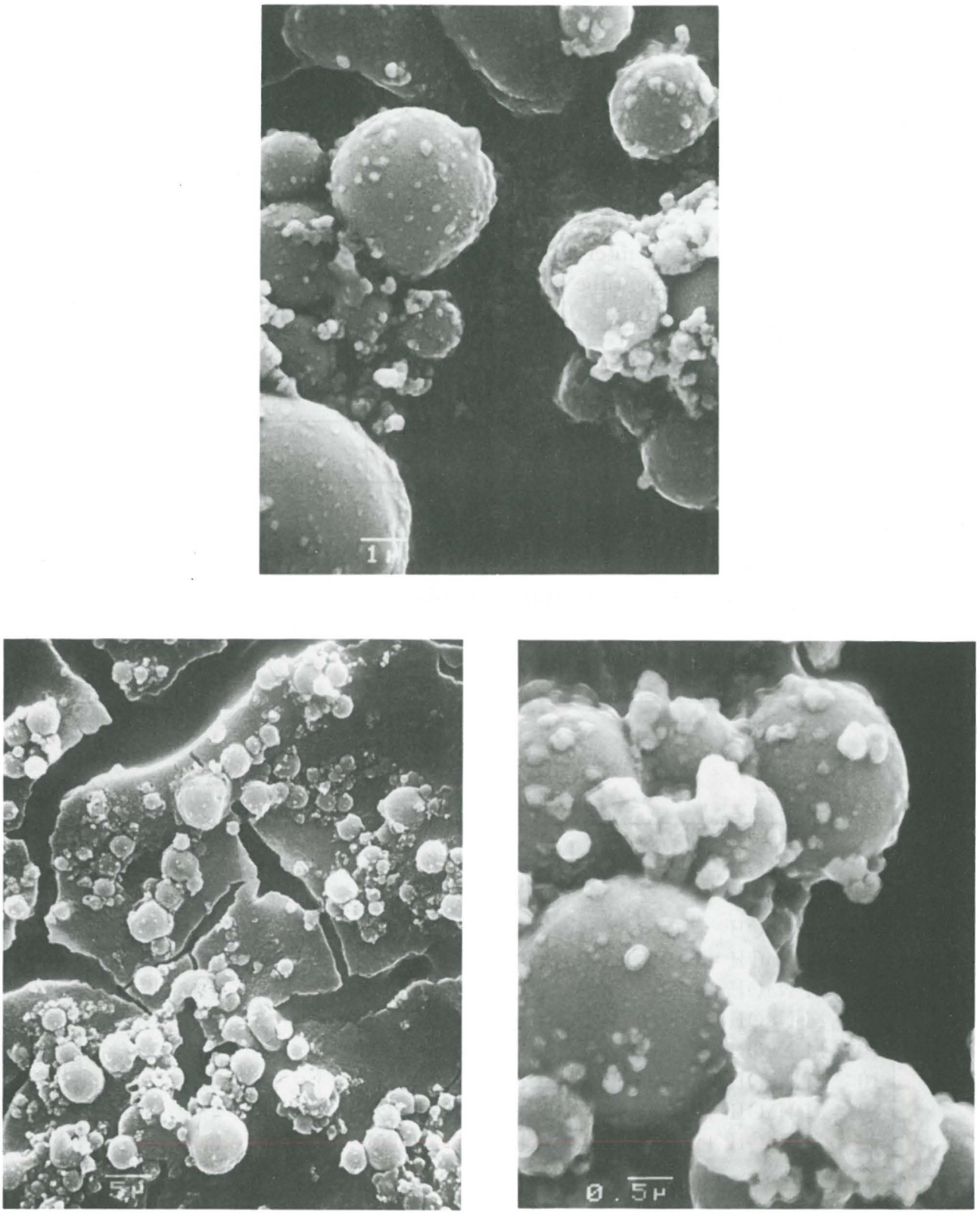

Figure 3.1: Scanning electron micrograph of a bitumen – in – water emulsion.

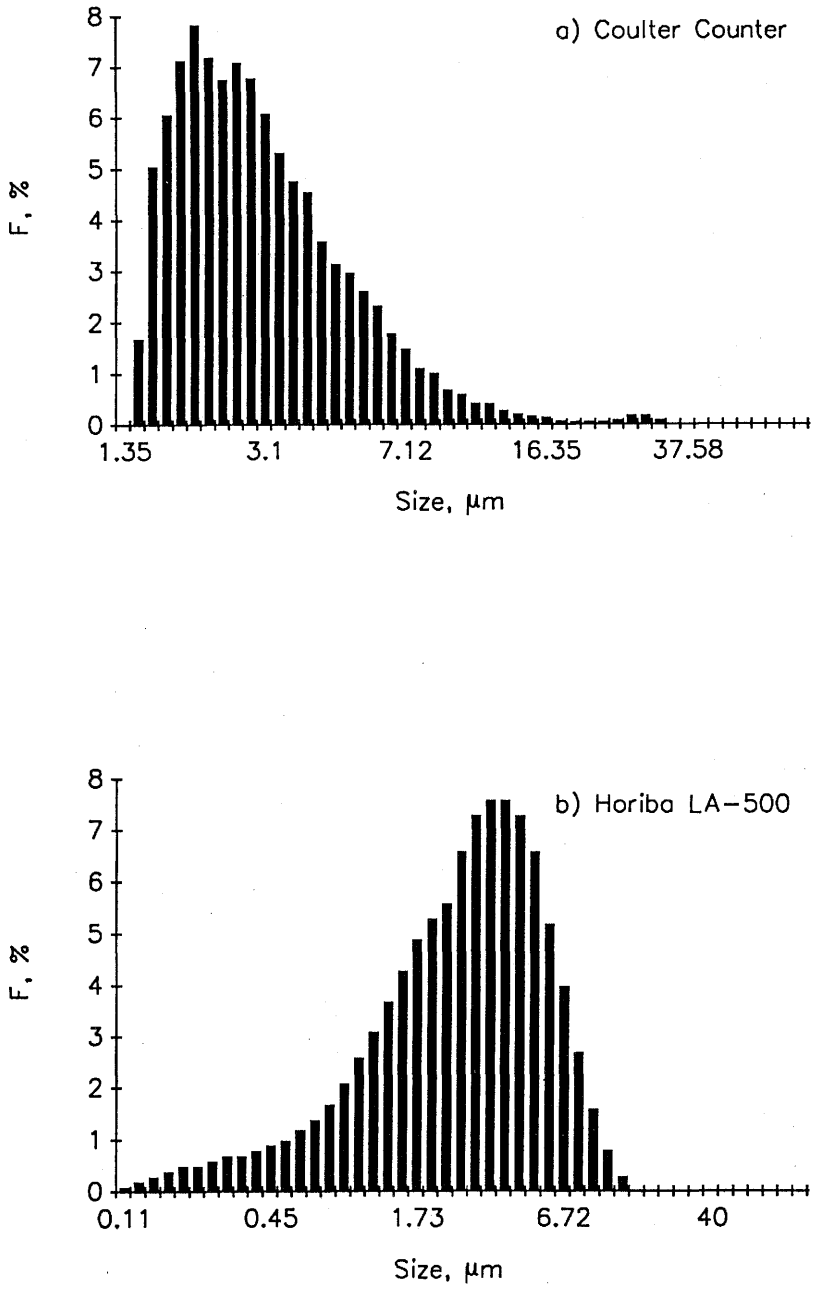

Figure 3.2: Particle Size Distribution of a bitumen/water emulsion measured by
a) Coulter Counter with a 70 μm orifice tube
b) Laser Diffraction Particle Size Analyzer (Horiba LA-500)

3.2.2 Dry weight determinations

Table 3.2 displays the dry weight and specific surface areas (SSA) for different bitumen emulsions. With the emulsifying procedure, described in section 3.1.1, it is possible to produce emulsions of a reproducible concentration of 0.2-0.3% (wt/wt) and a specific surface area of 3.5-4.5 m^2/g.

3.2.3 Surface group density

Figure 3.3 shows the adsorption isotherm of $Co(NH_3)_6^{3+}$ on bitumen. The adsorption isotherm shows a maximum adsorption level of 2.3±0.4 $\mu eq/m^2$. This corresponds to the total amount of carboxyl groups on the surface. In section 2 we noted that at pH=11 and I = 0.001 M, the dissociation of the carboxyl groups is almost complete. Further, $Co(NH_3)_6^{3+}$ reduces the surface potential, so that a complete deprotonation occurs at a pH value lower than shown in Fig. 2.1. The maximum adsorption level of $Co(NH_3)_6^{3+}$ thus indeed represents the total amount of surface groups. Our results are in good agreement with values reported in the literature [26]. The reported values, however, were not determined directly but were estimated by modelling experimental results of electrophoretic movement of bitumen particles.

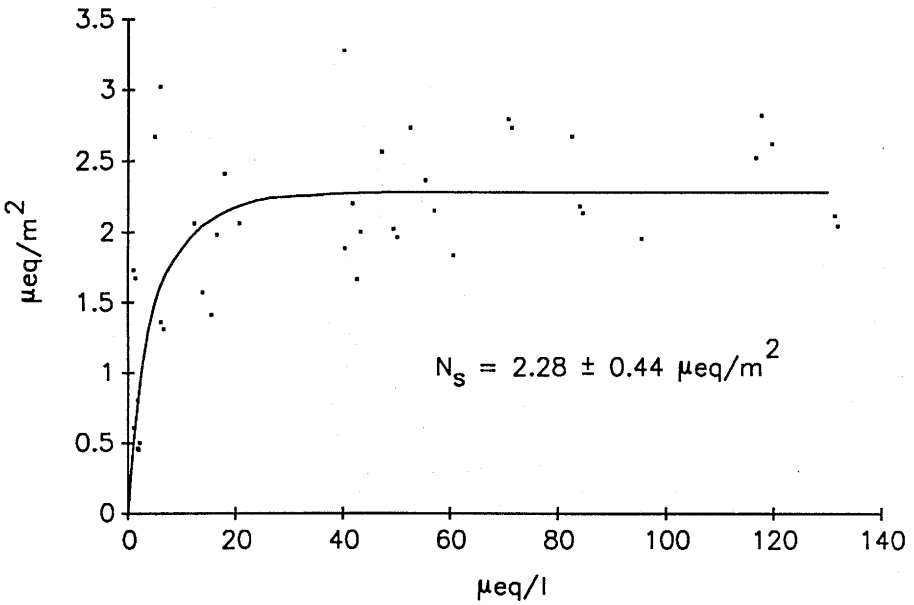

Figure 3.3: Adsorption isotherm of $Co(NH_3)_6^{3+}$ on bitumen at pH=11 (NaOH 10^{-3} M, T = 20°C)
N_s = 2.3±0.4 $\mu eq/m^2$ = $1.37 \cdot 10^{18}$ groups/m^2

4 Adsorption of Cs^+ on bitumen and latex

It was not possible to measure any degree of adsorption of $^{134}Cs^+$ on bitumen. This, however, does not mean that adsorption does not occur: it was just not measurable under the experimental conditions used in our experiments. The low concentration of bitumen (0.2–0.3 %) and the low specific surface area (3.5–4.5 m^2/g) resulted in a very low concentration of the active groups in the emulsion so that the adsorption of a weakly sorbing element like Cs^+ could not be measured.

In order to evaluate the adsorption of Cs^+ on bitumen and to estimate interaction constants, adsorption of Cs^+ on a carboxylated latex was studied. It is known from the literature that carboxylated latex (with the same surface group density) has about the same electric properties as bitumen (latex has a lower zeta potential due to surface roughness) and that the electric properties of the latex/water interface can also be explained well by the Ionizable Surface Group model [6,7]. It can therefore be used to evaluate the interaction between Cs^+ and a surface carboxyl group and to determine interaction constants for the Cs-carboxyl group interaction.

4.1 Materials and methods

4.1.1 Preparation and conditioning of latex suspensions

A well-defined carboxylated styrene-butadiene copolymer was used (Dow Europe). The most important characteristics have been summarized in Table 4.1.
30 ml aliquots of the latex suspension (50%) were placed in a dialysis bag (Dialysis Tubing-Visking, Medicell London) and dialysed 1 time against 1 L of 10^{-2} M NaOH and 5 times against 10^{-3} M NaOH (pH=11). Calculations with the Ionizable Surface

Table 4.1: Properties of the styrene butadiene copolymer suspension used in the Cs-adsorption experiments

Solid content	50%
pH	6.5 - 7.5
Particle size	138 ±10 nm
Specific Surface Area	43.6 m^2/g
Surface Group density	$1.84 \cdot 10^{18}$ groups/m^2
Density (suspension)	1 g/cm^3
Density (solid)	1 g/cm^3
Surface group	carboxyl group
Type	XZ 94301.70

Group model indicated that under these conditions (pH=11, I=0.001 M) the carboxyl groups were completely deprotonated and the latex was converted in the Na^+-form.

4.1.2 Determination of the functional group density by $Co(NH_3)_6^{3+}$

The suspension, prepared as described in 4.1.1 was diluted 10 times with 10^{-3} M NaOH. 10 ml aliquots of the diluted solution (2.71% dry weight) were placed in a 50 ml centrifuge tube and different volumes of a 10^{-2} N $Co(NH_3)_6^{3+}$ solution were added to it. The volume was made up to 30 ml with 10^{-3} M NaOH. The suspensions were shaken for 24 hours at room temperature. After equilibration, they were centrifuged at 11000 g for 30 minutes and the supernatant was analyzed for Co and Na by ICP-AES. The amount of $Co(NH_3)_6^{3+}$ adsorbed, and Na^+ desorbed, could be calculated from the difference in concentration before and after equilibrium.

4.1.3 Determination of the functional group density by isotopic exchange of $^{22}Na^+$

The Ionizable Surface Group model showed that at pH=11 and I=0.001 M, all the surface carboxyl groups are deprotonated and that the surface charge is completely neutralized by the Na^+ ions in the diffuse double layer. Under these conditions, the amount of surface groups can be determined by isotopic exchange of $^{22}Na^+$. The method is based on the fact that the distribution of $^{22}Na^+$ between the solid and liquid phase reflects the distribution of stable Na^+.

Consider the following ion exchange reaction:

$$\overline{Na^+} + {}^{22}Na^+ \rightleftharpoons \overline{{}^{22}Na^+} + Na^+ \qquad (10)$$

where the bar denotes the ions in the adsorbed phase.
The selectivity coefficient is defined as:

$${}^{22Na}_{Na}K_c = \frac{z_{{}^{22}Na} \cdot [Na^+]}{z_{Na} \cdot [{}^{22}Na^+]} \qquad (11)$$

where $z_{{}^{22}Na}$ and z_{Na} are the fractional occupancy of the CEC with $^{22}Na^+$ and Na^+. $[^{22}Na^+]$ and $[Na^+]$ are the concentration of $^{22}Na^+$ and Na^+ in the liquid phase.

Equation (11) can be rewritten as:

$${}^{22Na}_{Na}K_c = \frac{\overline{{}^{22}Na}/CEC \cdot [Na^+]}{z_{Na} \cdot [{}^{22}Na^+]} \qquad (12)$$

The concentration of $^{22}Na^+$ is much lower than the concentration of stable Na^+ so that z_{Na} approximately equals to 1.

With $\overline{^{22}Na}/[^{22}Na] = R_a^{^{22}Na}$ and z_{Na}=1, equation (12) is converted to:

$$^{^{22}Na}_{Na}K_c = \frac{R_a^{^{22}Na} \cdot [Na^+]}{CEC} \tag{13}$$

where CEC = cation exchange capacity (μeq/cm^2)
$R_a^{^{22}Na}$ = concentration ratio of ^{22}Na (cm)
$[Na^+]$ = concentration of Na^+ in solution (μeq/cm^3)

Equation (13) forms the basis for the determination of the surface group density (CEC).

$$^{^{22}Na}_{Na}K_c \cdot CEC = R_a^{^{22}Na} \cdot [Na^+] \tag{14}$$

Assuming to isotopic distribution, the value of $^{^{22}Na}_{Na}K_c$ equals 1 and equation 14 takes the form:

$$CEC = R_a^{^{22}Na} \cdot [Na^+] \tag{15}$$

When the concentration of Na^+ in solution is fixed at 10^{-3} M (1 μeq/cm^3), the value of the concentration ratio $R_a^{^{22}Na}$ equals the CEC or the amount of functional groups on the surface expressed as μeq/cm^2.
The latex solution prepared in section 4.1.1 was diluted 10 times with 10^{-3} M NaOH. 5 ml of the diluted solution were placed in a dialysis bag and equilibrated with 10^{-3} M NaOH.
15 ml of 10^{-3} M NaOH were brought in a 50 ml centrifuge tube and 5 ml of a 10^{-3} M NaOH solution, spiked with $^{22}Na^+$, were added. The 5 ml dialysis bags, containing the latex, were immersed in these solutions and shaken end-over-end for 24 hours. Reference systems containing dialysis bags without latex were set up simultaneously to evaluate the adsorption of $^{22}Na^+$ on the bags. After equilibrium, the outer solution was sampled and ^{22}Na was determined by liquid scintillation counting (Packard, Tricarb 2250 CA) using Instagel (Packard) as a scintillation cocktail.

4.1.4 Adsorption of Cs^+ on latex

The latex solution prepared in section 4.1.1 was diluted 10 times with 10^{-3} M NaOH. 5 ml of the diluted solution were placed in a dialysis bag and equilibrated 3 times with 10^{-3} M NaOH containing different concentrations of $NaClO_4$. The final concentration of Na^+ varied between 10^{-3} M and 10^{-2} M and the pH was 11. 15 ml solution with the same composition were brought in a centrifuge tube and 5 ml of solution spiked with carrier free $^{134}Cs^+$ were added. The concentration of Cs^+ was 10^{-8} M. Finally, the dialysis bags with latex were immersed in these solutions and the systems were shaken end-over-end for 24 hours at room temperature. After equilibrium, the outer solution was sampled and analyzed for ^{134}Cs by liquid scintillation counting. Reference systems containing dialysis bags only were set up simultaneously to evaluate the adsorption of $^{134}Cs^+$ on the bags.

The same procedure was repeated with Na^+ replaced by K^+ in order to study the effect of K^+ on the adsorption of Cs^+. Latex was thus converted in the K^+ form by 10^{-3} M KOH and the total K^+ concentration was varied between 10^{-3} M and 10^{-2} M using KNO_3.

4.2 Results and discussion

4.2.1 Surface group density

Figure 4.1 displays the adsorption isotherm of $Co(NH_3)_6^{3+}$ on latex. The maximum adsorption amounts to 6.0±0.1 μeq/m^2 and this corresponds to the density of functional groups on the surface. The amounts of Na^+ displaced from the solid phase are also given in Fig. 4.1 and equal 5.2±0.1 μeq/m^2, or 15% lower than the amount of $Co(NH_3)_6^{3+}$ adsorbed.

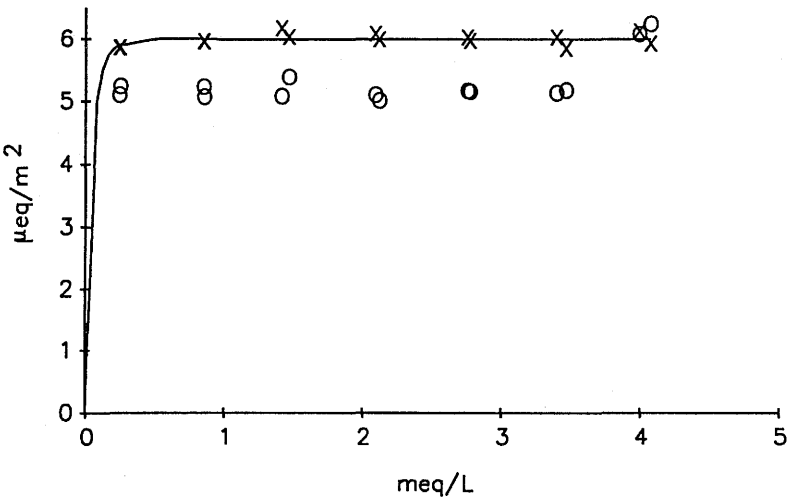

Figure 4.1: Adsorption isotherm of $Co(NH_3)_6^{3+}$ on latex (x). Desorption of Na^+ (o)

A possible explanation for this difference could be the fact that not all the carboxyl groups were deprotonated and converted to the Na^+ form by the prior treatment with 10^{-3}M NaOH. Indeed, Maes et al. [16] and Tits [29] have shown, for humic acids, that the charge measured by $Co(NH_3)_6^{3+}$ adsorption only identifies with the charge calculated from acid-base titrations at high ionic strength (about 3 M). At lower ionic strength, less functional groups are dissociated and are measurable in acid-base titrations.

Calculations with the Ionizable Surface Group model, however, predict that at pH=11 and I=0.001 M all carboxyl groups are deprotonated (assuming a pK_H of 4.5). Apparently this explanation is therefore not acceptable.
The density of functional groups determined by the isotopic exchange of $^{22}Na^+$ equals 4.0 ± 0.2 μeq/m^2. This is about 67% of the value determined by $Co(NH_3)_6^{3+}$ and 80% of the value derived from the displaced Na^+. It is difficult to evaluate which value is the correct one.
The value of 4 μeq/m^2 was regarded as suitable because it agrees with the value given by the manufacturer. This value will be used for calculations in the following experiments.

4.2.2 Adsorption of Cs^+ on latex

Figure 4.2 illustrates the adsorption of Cs^+ as function of the Na^+ or K^+ concentration in the equilibrium solution. The concentration ratio (R_a^{Cs}) decreases with increasing Na^+ or K^+ concentration in the equilibrium solution. Na^+ and K^+ compete with Cs^+ for adsorption on the carboxyl groups.

The experimental data can be explained well by an ion exchange mechanism. Consider the following homovalent ion exchange reaction:

$$\overline{M^+} + Cs^+ \rightleftharpoons M^+ + \overline{Cs^+} \tag{16}$$

in which the bar denotes the ions in the adsorbed phase.
The selectivity coefficient ${}^{Cs}_{M}K_c$ of the reaction is defined by:

$${}^{Cs}_{M}K_c = \frac{z_{Cs} \cdot [M^+] \cdot \gamma_M}{z_M \cdot [Cs^+] \cdot \gamma_{Cs}} \tag{17}$$

where: z_{Cs} and z_M = the fractional occupancy of the CEC by Cs^+ or M^+
$[Cs^+]$ and $[M^+]$ = the concentration of Cs^+ or M^+ in solution (μeq/cm^3)
γ_M and γ_{Cs} = the activity coefficient of M^+ or Cs^+ in solution

with : $M^+ = Na^+$ or K^+.

Since we are dealing with a system containing a macroelectrolyte M^+ and a trace element Cs^+ and the external solution is diluted, the aqueous-phase activity coefficient ratio γ_M/γ_{Cs} is essentially constant and equals 1 in the ionic strength range covered in our experiments. The concentration of the macroelectrolyte counterion on the surface is also constant, and equals the CEC. Under these conditions, the ratio of the latex phase activity coefficients is constant and is included in K_c [10].

Equation (17) can be written as:

$$ {}^{Cs}_{M}K_c = \frac{\overline{Cs^+}/CEC \cdot [M^+]}{z_M \cdot [Cs^+]} \tag{18} $$

with $\overline{Cs^+}$ = amount of Cs^+ adsorbed (μeq/cm^2)
CEC = cation exchange capacity (μeq/cm^2)

As the amount of Cs^+ (^{134}Cs) used is very low with respect to Na^+ or K^+ in the system, the composition of the latex surface does not change significantly when Cs^+ adsorbs. Consequently, the value of z_M is approximately equal to 1.
With $R_a^{Cs} = \overline{Cs}^+/[Cs^+]$, equation (18) is converted to:

$$ {}^{Cs}_{M}K_c(z_{Cs} \rightarrow 0) = \frac{R_a^{Cs} \cdot [M^+]}{CEC} \tag{19} $$

or

$$ R_a^{Cs} = \frac{{}^{Cs}_{M}K_c \cdot CEC}{[M^+]} \tag{20} $$

Equation (20) is thus only valid for the situation where z_M can be regarded to be 1.
Equation (20) shows that the concentration ratio depends on the functional group density (CEC), the selectivity coefficient and the concentration of competing ions in solution.
The solid lines in Fig. 4.2 show the evolution of the R_a^{Cs} as a function of the Na^+ or K^+ concentration in the liquid phase as calculated by equation (20). The value of ${}^{Cs}_{M}K_c$ was derived from a least square fit and is given in table 4.2. The ion exchange model describes very well the behaviour of Cs^+ in presence of Na^+ and K^+. The interaction of Cs^+ with the carboxyl group (and Na^+ or K^+ with a carboxyl group) is a pure coulombic interaction and not a specific adsorption (surface complexation reaction). This was expected because it is known from the literature that Cs^+ and other alkali metals do not form stable complexes with ligands containing carboxyl groups [23].

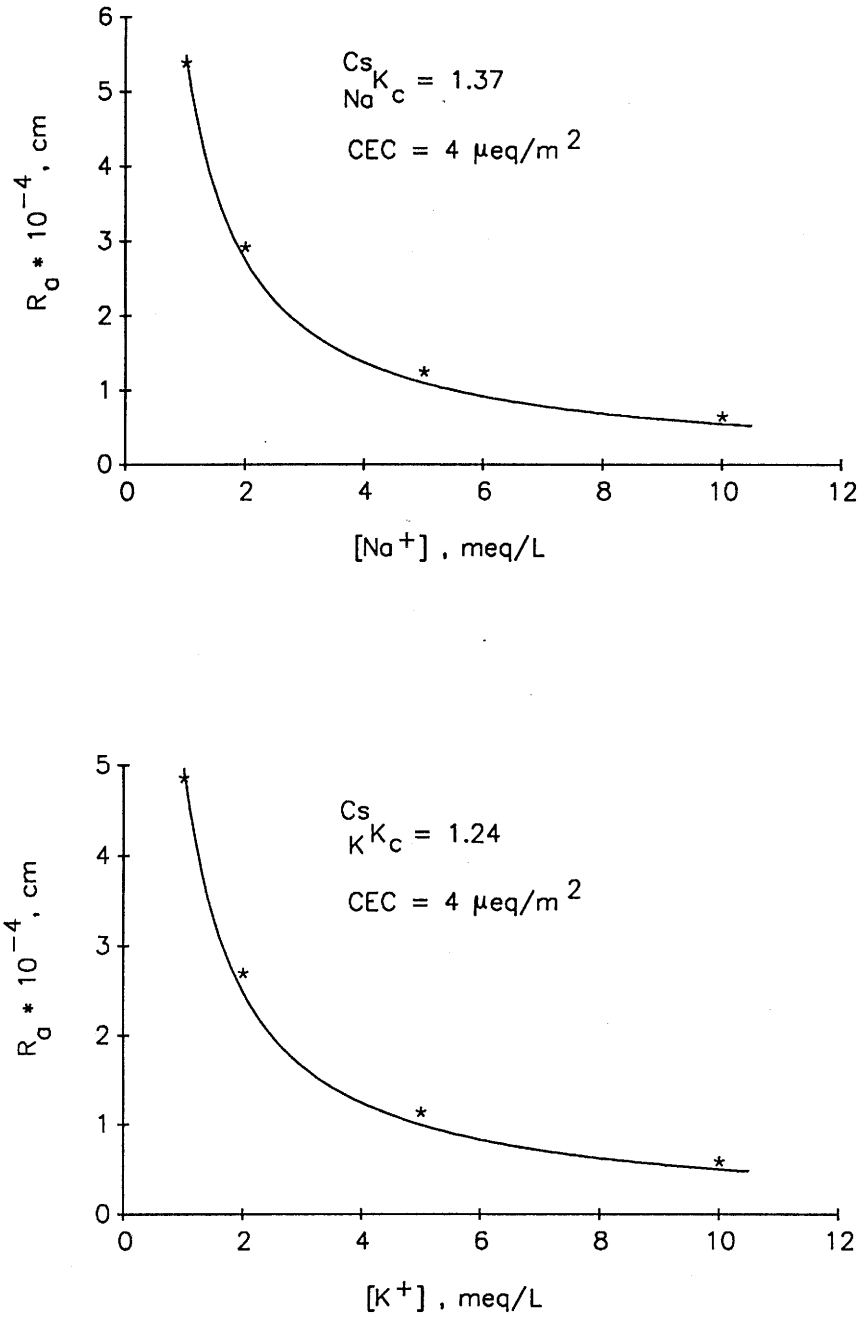

Figure 4.2: R_a (cm) values for Cs^+ on latex as function of the concentration of Na^+ or K^+ in the liquid phase
* experimental points – calculated by equation (20).

Table 4.2: Numerical values of the parameters used in equation (20)

CEC	$4 \cdot 10^{-4}$ μeq/cm^2
${}^{Cs}_{K}K_c$	1.24±0.03
${}^{Cs}_{Na}K_c$	1.37±0.03

Table 4.3: Overview of selectivity coefficient values for different carboxylated materials

	${}^{K}_{Na}K_c$	${}^{Cs}_{Na}K_c$	${}^{Cs}_{K}K_c$
Carboxylated Styrene-Butadiene (1)	1.10*	1.37	1.24
Polymethacrylate (2)	1.26*	2.50*	1.99*
Polyacrylate (3)	1.32*	1.86*	1.41*

(1) Ion exchange on K^+ or Na^+ loaded latex.
(2) Ion exchange on Li^+ loaded polymethacrylate.
(3) Ion exchange on NH_4^+ loaded polyacrylate.
(*) Calculated by applying Hess's law.

Table 4.2 also shows that the affinity of the different metals for the surface carboxyl groups is:

$$Cs > K > Na$$

Different affinity sequences can be explained by the interaction of the ions with the exchanger (electrostatic) and with the solvent (hydration) [11]. The latex seems to

have a normal behaviour. This means that hydration forces determine the overall free energy of exchange. The same selectivity series is observed for the weak acid exchange resins for which the selectivity coefficient data are given in table 4.3 [15]. Other selectivity series were also observed [22] in resins containing carboxylic groups with various specific capacities and degrees of cross-linking.

The numerical values of the selectivity coefficients [15] are comparable with the values observed for the carboxylated latex. The values of K_c, therefore, may be taken as typical for a carboxyl group and can, in general, be regarded as being independent of the matrix to which the carboxyl group has been fixed. Consequently, the selectivity coefficients found for latex or for carboxylated ion exchange resins can be used to evaluate the adsorption of Cs^+ on bitumen and to calculate R_a^{Cs} values under in situ conditions.

4.2.3 Evaluation of the adsorption of Cs^+ on bitumen under near field conditions

Equation (20) forms the basis for the estimation of the adsorption of Cs^+ on bitumen in a cementitious environment. It is assumed that the bitumen is in contact with a cement pore water having a composition given in Table 4.4 [2]. Na^+ and K^+ are the dominant cations present in this solution. At a pH of 13.2, all the surface carboxyl groups will be deprotonated and converted to the M^+ form (Na^+ and K^+).

Table 4.4: Composition of a Swedish standard Portland cement water SPP [2]

Parameter	Cement SPP
Temperature [°C]	25
pH	13.2
Ionic strength [M]	0.23
E_h (mV)	+139
Na^+ [M]	6.52×10^{-2}
K^+ [M]	1.61×10^{-1}
Mg^{2+} [M]	1.00×10^{-5}
Ca^{2+} [M]	2.25×10^{-3}
Fe_{tot} [M]	1.00×10^{-5}
Al [M]	2.00×10^{-4}
Alkalinity [N]	2.31×10^{-1}
SiO_2 [M]	2.00×10^{-4}

As the ${}^{Cs}_{Na}K_c$ and ${}^{Cs}_{K}K_c$ are about the same, a mean value of 1.3 can be used for the calculation. The CEC value, as determined in section 3, amounts $2.3{\cdot}10^{-4}$ μeq/cm^2. The concentration of M^+ is the sum of Na^+ and K^+ and equals 226.2 μeq/cm^3. The activity coefficient ratio γ_M/γ_{Cs} at an ionic strength of 0.23 M approximately equals 1 and can be neglected.

$$R_a^{Cs} = \frac{1.3 \cdot 2.28 \cdot 10^{-4}}{226.2} = 1.3 \cdot 10^{-6} \text{ cm} \approx 10^{-6} \text{ cm}$$

The competitive effect of Ca^{2+} (present at levels of $2{\cdot}10^{-3}$ M) has not been taken into account. As the competition of Ca^{2+} is much larger than Na^+ and K^+, one can conclude that the R_a^{Cs} in such environments would be $< 10^{-6}$ cm.

A value of 10^{-6} cm is very low and we can conclude that Cs^+ does not adsorb significantly on a bitumen surface in contact with a cement pore water due to the competition with Na^+, K^+ and Ca^{2+}.

5 The adsorption of Sr^{2+} on bitumen

5.1 Materials and methods

Bitumen emulsions were prepared as described in 3.1. The emulsions were placed in dialysis bags and equilibrated with 10^{-3} M NaOH containing different $NaClO_4$ concentrations between 10^{-3} M and $9 \cdot 10^{-3}$ M. The total Na^+ concentration varied from 10^{-3} M to 10^{-2} M.
After equilibration, 20 ml aliquots of the bitumen emulsions were transferred to 50 ml centrifuge tubes (Oak Ridge Type, Teflon) and 5 ml of the equilibrium solution, spiked with $^{85}Sr^{2+}$, were added to it. The concentration of Sr^{2+} was 10^{-10} M. The mixtures were shaken end-over-end for 24 hours whereafter a phase separation was performed by centrifugation at 11000 g for 30 minutes. 2 ml of the clear supernatant were sampled and analyzed for ^{85}Sr by liquid scintillation counting (Packard, Tricarb 2250 CA) using Instagel (Packard) as scintillation cocktail. The amount of Sr^{2+} adsorbed was calculated from the difference in concentration before and after equilibrium.

To study the pH dependency of the Sr^{2+}-adsorption, bitumen emulsions were equilibrated in dialysis bags at different pH values between 7 and 11. Because of the low buffering capacity of the bitumen emulsion, $5 \cdot 10^{-4}$ M TRIS (Tris (hydroxy methyl)-aminomethane) was used to buffer the pH in the range 7 to 8.6. Beyond pH 9, the pH was adjusted by NaOH. The same adsorption procedure was used as described earlier.

The effect of complexing substances on the adsorption of Sr^{2+} on bitumen was studied by adding NTA (nitrilotriacetic acid) to the liquid phase. NTA builds 1:1 complexes with Sr^{2+} of intermediate stability. The concentration of NTA was varied from 10^{-6} M to 10^{-4} M. The total Na^+ concentration was fixed at $1.5 \cdot 10^{-3}$ M and the pH at 11. The adsorption was performed in the same way as described above.

5.2 Results and discussion

5.2.1 The adsorption of Sr^{2+} as a function of Na^+ in the liquid phase

Figure 5.1 displays the adsorption of $^{85}Sr^{2+}$ (R_a^{Sr}, cm) as function of the Na^+ concentration in the equilibrium solution. The concentration ratio decreases with increasing Na^+ concentration in the equilibrium solution.
Initially, the adsorption of Sr^{2+} was assumed to be an ion exchange process given by the following heterovalent ion exchange reaction:

$$2\overline{Na}^+ + Sr^{2+} \rightleftharpoons \overline{Sr^{2+}} + 2Na^+ \qquad (21)$$

The selectivity coefficient is defined by:

$$ {}^{Sr}_{Na}K_c = \frac{z_{Sr} \cdot [Na^+]^2 \cdot \gamma_{Na}^2}{z_{Na}^2 \cdot [Sr^{2+}] \cdot \gamma_{Sr}} \tag{22} $$

with : z_{Sr} and z_{Na} = fractional occupancy of the surface by Sr^{2+} and Na^+
$[Sr^{2+}]$ and $[Na^+]$ = the concentration of Sr^{2+} and Na^+ in solution (μmol/cm^3)
γ_{Na} and γ_{Sr} = the activity coefficient of Na^+ and Sr^{2+} in solution

Since we are dealing with a system containing a macroelectrolyte Na^+ and a trace element Sr^{2+}, the composition of the bitumen surface does not change significantly when Sr^{2+} adsorbs. The activity coefficient ratio of the adsorbed species is constant and is included in the ${}^{Sr}_{Na}K_c$ value. The aqueous activity coefficient ratio can be calculated from the extended Debye-Huckel theory [20] and is denoted by Γ in the subsequent equations.
The term z_{Sr} can be replaced by $\overline{Sr}$/CEC:

$$ {}^{Sr}_{Na}K_c = \frac{\overline{Sr}/CEC \cdot [Na^+]^2}{z_{Na}^2 \cdot 2 \cdot [Sr^{2+}]} \cdot \Gamma \tag{23} $$

with $\Gamma = \gamma_{Na}^2/\gamma_{Sr}$.
The factor 2 in equation (23) is introduced because the concentration of Sr^{2+} on the surface is expressed on equivalent basis.
Since z_{Na}=1 at trace level occupancy of Sr^{2+} and $\overline{Sr}/(2 \cdot [Sr^{2+}]) = R_a^{Sr}$ (cm), equation (23) can be written as:

$$ {}^{Sr}_{Na}K_c(z_{Sr} \rightarrow 0) = \frac{R_a^{Sr} \cdot [Na^+]^2}{CEC} \cdot \Gamma \tag{24} $$

or

$$ R_a^{Sr} \cdot \Gamma = \frac{{}^{Sr}_{Na}K_c \cdot CEC}{[Na^+]^2} \tag{25} $$

$$ log(R_a^{Sr} \cdot \Gamma) = log {}^{Sr}_{Na}K_c + log\ CEC - 2 \cdot log[Na^+] \tag{26} $$

In case of a pure ion exchange process, the log–log plot of ($R_a^{Sr} \cdot \Gamma$) as a function of [Na^+] yields a straight line with a slope –2. Figure 5.2 represents such a log–log plot.

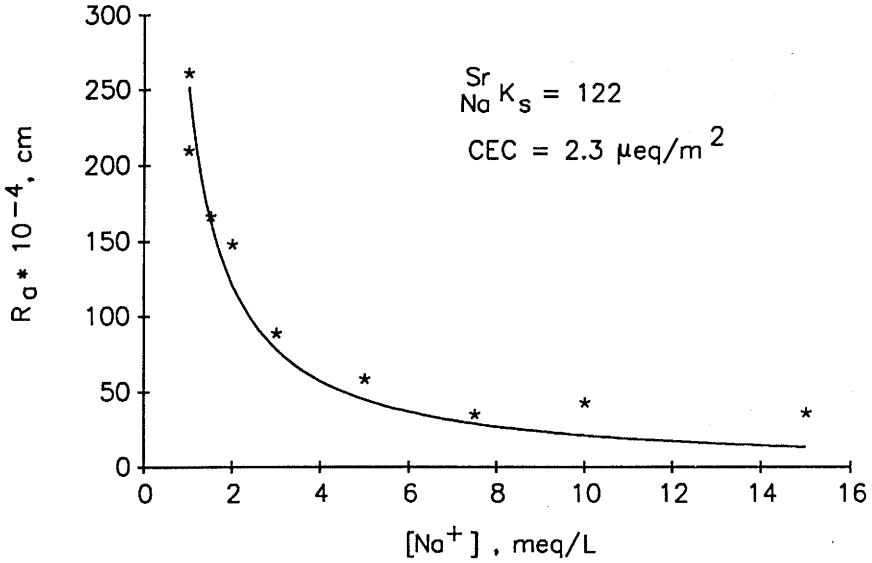

Figure 5.1: Adsorption of Sr^{2+} on bitumen as a function of the Na^+ concentration in the liquid phase
$*$: experimental points, – : calculated by equation (30)

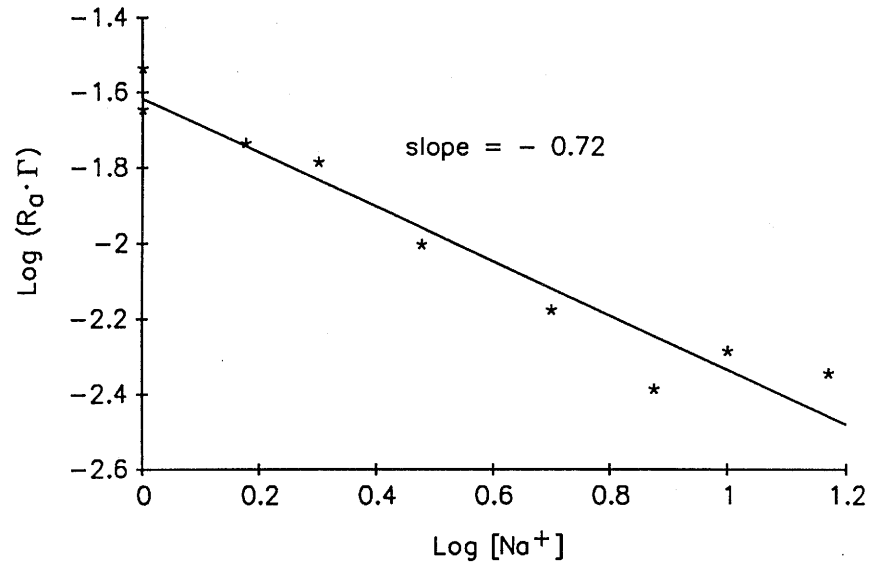

Figure 5.2: Log–log plot of $R_a^{Sr} \cdot \Gamma$ as a function of $[Na^+]$
$*$: experimental points; – : linear regression analysis

The slope of the straight line equals –0.72 instead of –2. When neglecting the data of the two highest Na^+ concentrations, the log–log plot has a slope of –0.89. As this is close to –1, it can be concluded that 1 mol of Na^+ is exchanged by 1 mol of Sr^{2+}. PHREEQE calculations showed that at pH 11 = 11, 99.6 % of the strontium is present as Sr^{2+} and only 0.4 % as $SrOH^+$. Consequently, strontium indeed adsorbs as Sr^{2+} and not as $Sr(OH)^+$ on the bitumen. This observation suggests that the adsorption of Sr^{2+} on bitumen is not a pure ion exchange process, but has a specific interaction character. If we assume that the reaction of Sr^{2+} with the bitumen surface (carboxyl group) can be written as:

$$RCOONa + Sr^{2+} \rightleftharpoons RCOOSr^+ + Na^+ \tag{27}$$

then

$$^{Sr}_{Na}K_s = \frac{\{RCOOSr^+\} \cdot [Na^+] \cdot \gamma_{Na}}{\{RCOONa\} \cdot [Sr^{2+}] \cdot \gamma_{Sr}} \tag{28}$$

Since we are dealing with trace amounts of Sr^{2+}, the composition of the surface does not change significantly when Sr^{2+} adsorbs. The surface charge and potential are completely determined by the pH and the Na^+ concentration. Consequently, $\{COONa\}$ equals the actual CEC of the bitumen.
As $R_a^{Sr} = \{RCOOSr^+\}/[Sr^{2+}]$, equation (28) takes the form:

$$^{Sr}_{Na}K_s(z_{Sr} \rightarrow 0) = \frac{R_a^{Sr} \cdot [Na^+]}{CEC} \cdot \Gamma \tag{29}$$

and

$$R_a^{Sr} = \frac{^{Sr}_{Na}K_s \cdot CEC}{[Na^+] \cdot \Gamma} \tag{30}$$

where $\Gamma = \gamma_{Na}/\gamma_{Sr}$

$$log(R_a^{Sr} \cdot \Gamma) = log(^{Sr}_{Na}K_s \cdot CEC) - \log[Na^+] \tag{31}$$

A log–log plot of ($R_a^{Sr} \cdot \Gamma$) as function of [Na^+] has to yield a straight line with slope –1. Figure 5.3 shows such a plot. The plot indeed yields a straight line with a slope equal to –0.69. Neglecting the points at the two highest concentrations of Na^+, the slope is –0.86, which is close to –1. The solid line in Fig. 5.1 shows a least square fit of the experimental R_a^{Sr} by equation (30). The value of $^{Sr}_{Na}K_c$ derived from this least

square fit equals 122 ± 7. The value of the CEC was fixed at 2.3 μeq/m^2. Equation (30) describes the experimental data reasonably good.

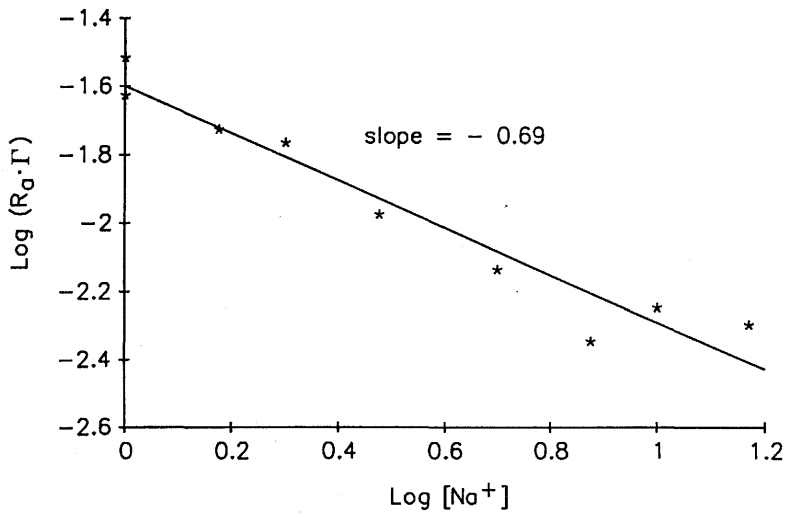

Figure 5.3: Log–log plot of $R_a^{Sr} \cdot \Gamma$ as a function of $[Na^+]$
$*$: experimental points; – : linear regression analysis

The model thus assumes that one carboxyl group reacts with one Sr^{2+} ion to form a surface complex or surface ion-pair (Fig. 5.4a). As the adsorption depends on the Na^+ concentration in solution, the complex is an outer-sphere complex. This means that the complex formation is caused by an electrostatic attraction between ligand and metal atom, both of which conserve their hydration sphere [4]. An analogue reaction has been reported in the literature for the adsorption of Ca^{2+} on bitumen [6].
Evidence for a complexation reaction with one surface carboxyl group is given by the surface group density. The density of functional groups equals $1.37 \cdot 10^{14}$ groups/cm^2 or 1.37 groups/nm^2. One carboxyl group is thus localized on a surface of 0.7 nm^2. The mean distance between two adjacent carboxyl groups equals ±0.9 nm, corresponding to 4 C-C bonds. This distance is too large to allow a chelation reaction with two carboxyl groups (Fig. 5.4b).
This evidence is also supported by the observation that the stability constants of complexes of bicarboxylic acids and metals decrease with increasing distance between the two carboxylic groups. As soon as the carboxyl groups are separated by two or more C-atoms, the stability constant is low and changes little with increasing distance [23].

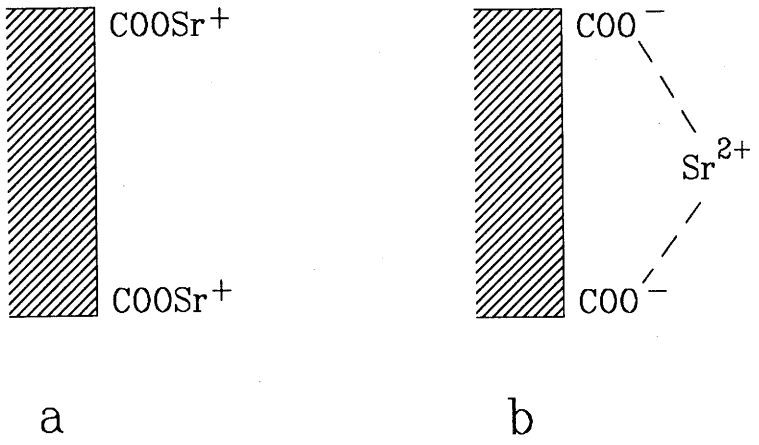

Figure 5.4: Surface complexation of Sr^{2+} with a carboxylic group.

5.2.2 The adsorption of Sr^{2+} on bitumen as function of the pH of the liquid phase

The model derived above, in fact, represents a limiting case where the CEC has reached its maximum value CEC_{max}. At lower pH values, fewer carboxyl groups are deprotonated, so that the adsorption is expected to be lower. Figure 5.5 displays the dissociation of carboxyl groups on bitumen as a function of pH for N_s=1.37·10^{18} groups/m^2 and pK_H=6.6. Figure 5.6 shows the adsorption of Sr^{2+} on bitumen (R_a^{Sr}) as a function of the pH of the liquid phase. As was expected, the adsorption is lower for lower pH values. Equation (30) has now to be modified to:

$$R_a^{Sr} = \frac{{}^{Sr}_{Na}K_s \cdot \alpha \cdot CEC_{max}}{[Na^+] \cdot \Gamma} \tag{32}$$

with $\alpha = -\sigma_o/eN_s$, denoting the fraction of carboxyl groups dissociated.

The value of σ_o can be calculated for specific pH and I values by applying equation (7), (8) and (9) from section 2.
The solid line in Fig. 5.6 shows the least square fit of the experimental data by equation (32). The value of pK_H was fixed at 6.6. ${}^{Sr}_{Na}K_s$ was obtained from the least square fit and equals to 139 ± 8. The value of the deprotonation constant pK_H was 6.6 in our calculations instead of the more common value 4.5-4.8, typical for COOH groups. This is in contradiction with results found by Takamura and Chow [26]. They assumed a value for pK_H of 4.5 for carboxyl groups on bitumen. A reasonable explanation for this difference can not be given at the moment because no information is available on the nature and chemical environment of the carboxyl groups. A value of 6.6, on the other hand, is not an implausible value. The pK_H values observed for the carboxyl groups of different compounds in solution have a Gaussian distribution, exhibiting values from 0.5 to 8.5 [21].
As shown in Fig. 5.5, the dissociation of the carboxyl groups (with $pK_H = 6.6$) at pH $\leq$ 11 depends on the ionic strength of the contact solution. This has, of course, consequences on the adsorption of Sr^{2+} at different ionic strength values. In section 5.2.1, the CEC was assumed to have its maximum value CEC_{max}. When this is not the case equation (32) has to be used instead of equation (30) to model the experimental data of section 5.2.1. The log–log plot of $(K_s^{Sr} \cdot \Gamma/CEC)$ as a function of [Na^+] has to yield a straight line with slope –1. Fig. 5.7 displays such a straight line with a slope of –0.78. When neglecting the the points at the two highest Na^+ concentrations, the slope increase to –0.96. The lower values of the slope observed earlier (fig. 5.2 and 5.3) can be explained by the fact that the CEC is not constant , but varies with the ionic strength at pH = 11. The slope of –0.96 is very close to –1 and makes the model acceptable.

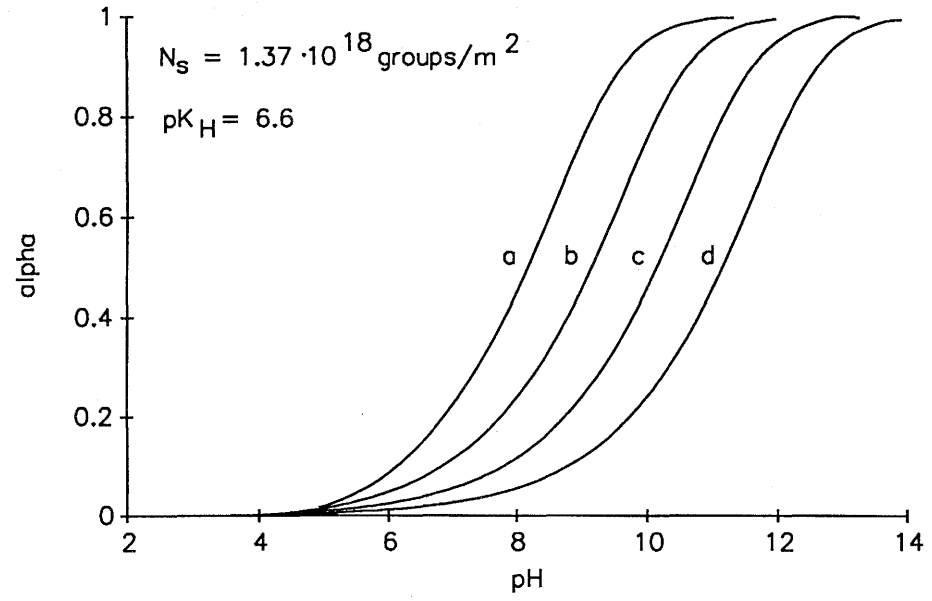

Figure 5.5: Deprotonation of surface carboxyl groups on bitumen as a function of pH
Surface group density: $1.37 \cdot 10^{18}$ groups/m^2; pK_H=6.6
a) I=0.1 M; b) I=0.01 M; c) I=0.001 M; d) I=0.0001 M

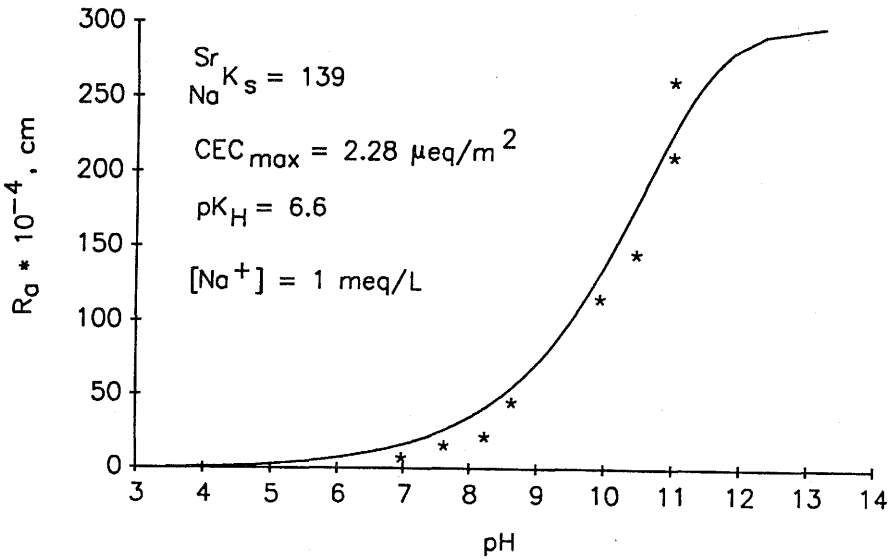

Figure 5.6: Adsorption of Sr^{2+} on bitumen as function of pH at I=0.001 M
$*$: experimental points; – : calculated by equation (32)

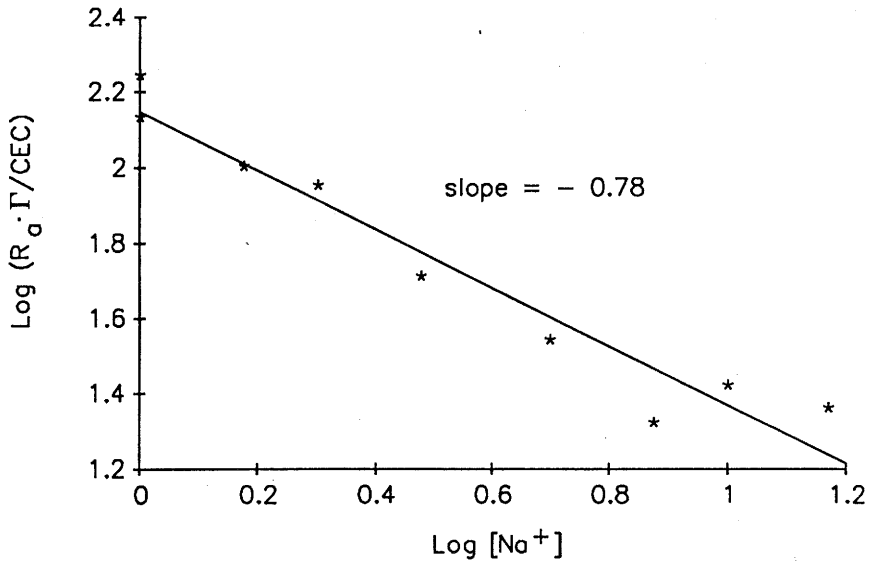

Figure 5.7: Log–log plot of $(R_a^{Sr} \cdot \Gamma/CEC)$ as a function of $[Na^+]$
$*$: experimental points; – : linear regression analysis

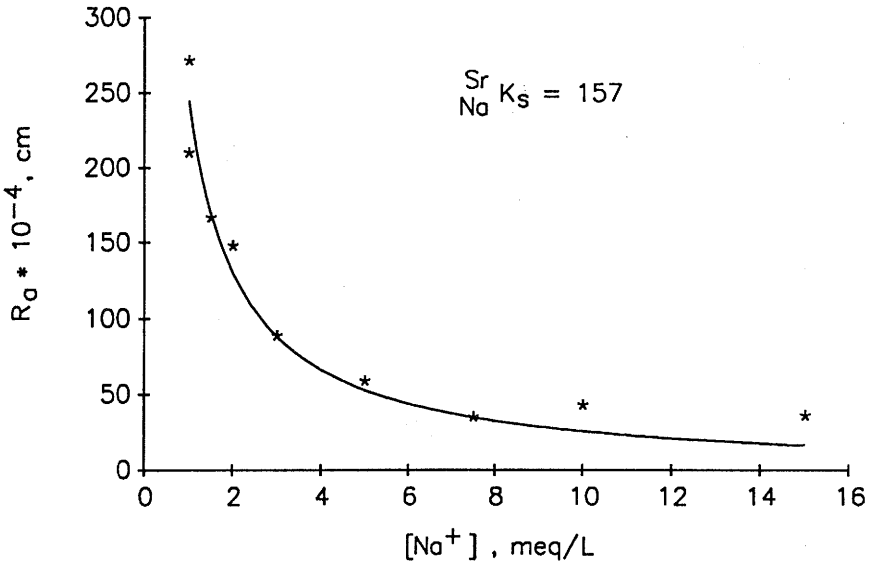

Figure 5.8: Adsorption of Sr^{2+} on bitumen as a function of the Na^+ concentration in the liquid phase
$*$: experimental points, – : calculated by equation (32)

The corrections introduced by this effect, however, are not very large. Fig. 5.8 shows the least square fit of the R_a^{Sr} data, obtained in section 5.2.1, by equation (32). The value for ${}^{Sr}_{Na}K_s$ derived from the least square fit equals 157 $\pm$ 7. The CEC values used for the fit were calculated, using equation (7), (8) and (9) to estimate α. Equation (32) describes the experimental data very well. The value of the surface complexation constant is somewhat larger and can be assumed to be more correct.

5.2.3 Adsorption of Sr^{2+} on bitumen in presence of complexing ligands

In the experiments and models described earlier, it was assumed that no complexation of Sr^{2+} occurs in the liquid phase. As soon as competing complexation reactions (hydrolysis, ion pair formation, complexation with humic acids and organics as EDTA, DTPA, NTA ....) occur in the liquid phase, the above derived models must be extended to account for this effect.

Assume the following complexation reaction taking place in the liquid phase:

$$Sr^{2+} + L^{2-} \rightleftharpoons SrL \tag{33}$$

The stability constant of the complex is defined as:

$$K_{SrL} = \frac{[SrL]}{[Sr^{2+}][L^{2-}]} \tag{34}$$

The total concentration of Sr is:

$$\begin{aligned} [Sr]_{tot} &= [Sr^{2+}] + [SrL] && (35)\\ &= [Sr^{2+}] + K_{SrL} \cdot [Sr^{2+}] \cdot [L^{2-}] && (36)\\ &= [Sr^{2+}](1 + K_{SrL} \cdot [L^{2-}]) && (37) \end{aligned}$$

The hydrolysis of Sr^{2+} can be neglected.

The adsorption of complexed Sr^{2+} is assumed not to take place because the adsorption is caused by a weak Coulombic interaction. The adsorption of Sr^{2+} can be written as:

$$RCOONa + Sr^{2+} \rightleftharpoons RCOOSr^{+} + Na^{+} \tag{38}$$

and the equilibrium constant is defined as:

$${}^{Sr}_{Na}K_s = \frac{\{RCOOSr^{+}\} \cdot [Na^{+}]}{\{RCOONa\} \cdot [Sr^{2+}]} \cdot \Gamma \tag{39}$$

$$\text{With :} \quad [Sr^{2+}] = \frac{[Sr_{tot}]}{(1 + K_{SrL}[L^{2-}])}$$

$$\text{and} \quad \{RCOONa\} = \text{CEC}$$

equation (39) is transformed in:

$$\overset{Sr}{_{Na}}K_s = \frac{R_a^{Sr} \cdot [Na^+]}{CEC/(1 + K_{SrL} \cdot [L^{2-}])} \cdot \Gamma \tag{40}$$

or

$$R_a^{Sr} = \frac{\overset{Sr}{_{Na}}K_s \cdot \alpha \cdot CEC_{max} \cdot}{[Na^+] \cdot (1 + K_{SrL} \cdot [L^{2-}]) \cdot \Gamma} \tag{41}$$

The adsorption of Sr^{2+} was studied in presence of NTA (Nitrilotriacetic acid). NTA builds 1:1 complexes with Sr^{2+} with a stability constant logK=5.0 (I=0.1 M) [23]. The adsorption experiments were carried out at pH=11 and a Na^+ concentration of 0.0015 M. The value of the stability constant of NTA with Sr^{2+} equals 5.2 at this ionic strength. At pH=11, 76% of the carboxyl groups are deprotonated (derived from Fig. 5.5) so that the CEC has a value of 1.73 μeq/m^2.

Figure 5.9 shows the adsorption of Sr^{2+} (expressed as R_a^{Sr}) as a function of the NTA concentration in solution. The figure clearly demonstrates the inhibiting effect of NTA on the adsorption of Sr^{2+}. The solid line in Fig. 5.9 represents a least square fit of the experimental R_a^{Sr} as by equation (41). The value of $\overset{Na}{_{Sr}}K_s$ derived from the least square fit equals 174 $\pm$ 9. Equation (41) describes very well the experimental results, proving the validity of the model. This is in fact not surprising because equation (41) forms the basis equation of the Schubert method for the determination of stability constants of complexes [30].
Equation (41) is a general equation that describes the adsorption of Sr^{2+} as a function of pH, ionic strength and concentration of complexing ligands in solution. Depending on the environmental conditions, equation (41) can be reduced to more simple equations. The values of $\overset{Sr}{_{Na}}K_s$ obtained from the different experiments are summarized in Table 5.1. The values are very similar and we can conclude that a value of 160 (logK = 2.2) characterizes the adsorption of Sr^{2+} in presence of Na^+ and K^+. In case of Ca^{2+} as counter-ion, the value of $\overset{Sr}{_{Ca}}K_s$ is expected to be 1 because of the similar chemistry of both Sr^{2+} and Ca^{2+}. Complexes of carboxylic acids with both Ca^{2+} and Sr^{2+} show similar stability constants [23].

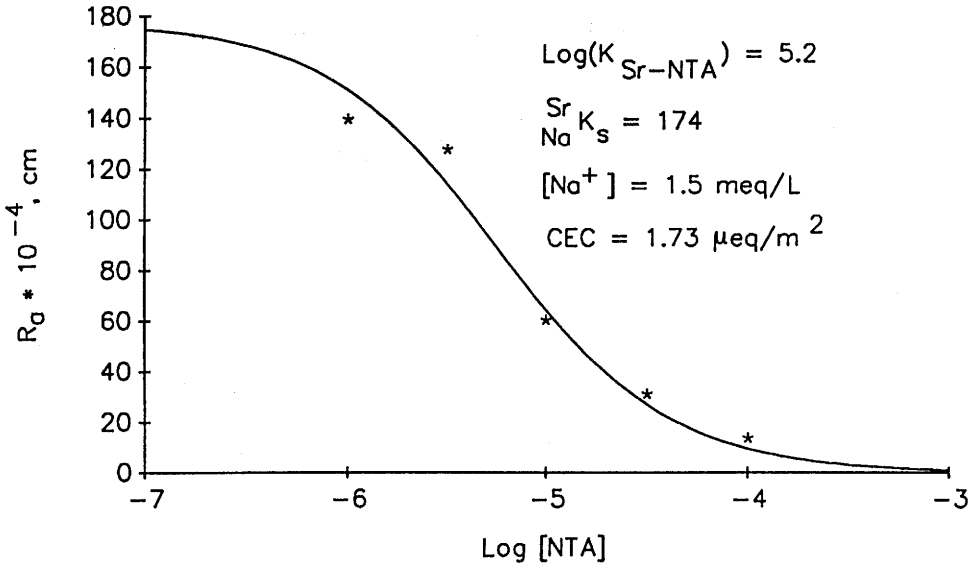

Figure 5.9: Adsorption of Sr^{2+} on bitumen at pH=11 and I=0.0015 M as a function of [NTA] in the liquid phase
$*$ experimental results; – calculated by applying equation (41)

Table 4.3: Overview of $^{Sr}_{Na}K_s$ values obtained from different experiments

Experiment	$^{Sr}_{Na}K_s$	$\log^{Sr}_{Na}K_s$
variable [Na^+]	157 ± 7	2.20
variable pH	139 ± 8	2.14
NTA	174 ± 9	2.24

5.3 Evaluation of the adsorption of Sr^{2+} on bitumen under near field conditions

Equation (41) can be used to calculate the adsorption (R_a^{Sr}) of Sr^{2+} on bitumen under near field conditions (cementitious environment). Under near field conditions, all the carboxyl groups are deprotonated ($\alpha = 1$) so that the CEC value takes its maximum value of 2.3 μeq/m^2. The hydrolysis reactions of Sr^{2+} becomes more important at this

high pH (Sr^{2+} : 80 % ; $Sr(OH)^{+}$: 20 %) but can be neglected because Sr^{2+} is still the dominant species. Equation (41) is thus reduced to its most simple form:

$$R_a^{Sr} = \frac{{}^{Sr}_{Na}K_s \cdot CEC_{max}}{[Na^+] \cdot \Gamma} \tag{42}$$

The ${}^{Sr}_{Na}K_s$ is expected to be the same as ${}^{Sr}_{K}K_s$ because Na^+ and K^+ show the same affinity for carboxyl groups (see Table 4.3). Consequently, equation (42) can be written as:

$$R_a^{Sr} = \frac{{}^{Sr}_{Na,K}K_s \cdot CEC_{max}}{([Na^+] + [K^+]) \cdot \Gamma} \tag{43}$$

The composition of a Swedish Standard cement pore water is given in Table 4.4 [2]. The activity coefficient ratio Γ equals 2.45 at an ionic strength of 0.22 M. A mean value of 160 for the ${}^{Sr}_{Na,K}K_s$ was taken. This value, of course, is a maximum value operating at trace levels of Sr^{2+}. At higher concentrations of Sr^{2+}, the value of ${}^{Sr}_{Na,K}K_s$ is expected to be lower because interaction of Sr^{2+} with less specific surface groups might occur when the loading of the bitumen surface with Sr^{2+} increases. The subsequent calculations thus represent the maximum R_a^{Sr} value that can be expected.
The value of R_a^{Sr} is calculated to be:

$$R_a^{Sr} = \frac{160 \cdot 2.28 \cdot 10^{-4}}{226.2 \cdot 2.45} = 7.0 \cdot 10^{-5} \text{ cm}$$

Taking the competitive effect of Ca^{2+} into account, one can predict that $R_a^{Sr} \leq 7 \cdot 10^{-5}$ cm. A value of 10^{-4} cm is a very low value and we can conclude that in a cementitious environment, Sr^{2+} does not adsorb to a large extend on the bitumen due to competition with Na^+, K^+ and Ca^{2+} present in the cement pore water.

6 Adsorption of Ni^{2+} on bitumen

6.1 Materials and methods

Bitumen emulsions were prepared as described in section 3.1.1. The emulsions were placed in dialysis membranes and equilibrated at the desired ionic strength and pH value. Between pH 7 and 9, the solutions were buffered with $5 \cdot 10^{-4}$ M TRIS. Beyond pH 9, the pH was adjusted by NaOH. The ionic strength was varied between 0.001 and 0.01 M by $NaClO_4$. 20 ml aliquots of the bitumen emulsion were transferred to 50 ml centrifuge tubes and 5 ml of the equilibrium solution, spiked with carrier free $^{63}Ni^{2+}$, were added. The final Ni^{2+} concentration was 10^{-8} M.
The mixtures were shaken end-over-end for 24 hours and afterwards centrifuged at 11000 g for 30 minutes. 2 ml of the clear supernatant were sampled and analyzed for ^{63}Ni by liquid scintillation counting (Packard, Tricarb 2250 CA) using Instagel (Packard) as scintillation cocktail. The adsorption (R_a^{Ni}) was calculated from the difference in concentration before and after equilibrium.
Blank tests without bitumen were setup in parallel to check the adsorption on the vessel walls.

6.2 Results and discussion

Figure 6.1 displays the adsorption of Ni^{2+} (R_a^{Ni}, cm) as a function of pH. As can be observed, the experimental data show a large spread. A few observations, however, are obvious. There is an increase in adsorption with increasing pH in the pH range 7-8.5. Beyond pH 11, no or very low adsorption can be observed. The increase in adsorption can be explained by an increase in the adsorption capacity (CEC) on the bitumen surface. The low adsorption at pH values >10.5 can be explained by the hydrolysis side reaction. The building of neutral $Ni(OH)_2^o$ or anionic $Ni(OH)_3^-$ and $Ni(OH)_4^{2-}$ species in solution competes with the adsorption of Ni^{2+} on the solid phase and makes adsorption impossible at higher pH values.
As Ni^{2+} forms relative stable complexes with i.a. carboxyl groups because of its partly unfilled d-orbitals, the adsorption of Ni^{2+} was assumed to be a surface complexation reaction :

$$Ni^{2+} + RCOO^- \rightleftharpoons RCOONi^+ \tag{44}$$

and is characterized by the equilibrium constant:

$$K_s^{Ni} = \frac{\{RCOONi^+\}}{\{RCOO^-\} \cdot [Ni^{2+}] \cdot \gamma_{Ni}} \tag{45}$$

The adsorption of complexed Ni^{2+} is assumed to be negligible. In cases where complexation or hydrolysis reactions occur, these reactions have to be combined with the adsorption reaction.

Assume the following reactions of Ni^{2+} occuring in solution:

$$Ni^{2+} + L^{2-} \rightleftharpoons NiL \tag{46}$$

with

$$K_{NiL} = \frac{[NiL]}{[Ni^{2+}] \cdot [L^{2-}]} \tag{47}$$

and

$$Ni^{2+} + OH^- \rightleftharpoons NiOH^+ \tag{48}$$

$$Ni^{2+} + 2OH^- \rightleftharpoons Ni(OH)_2^\circ \tag{49}$$

$$Ni^{2+} + 3OH^- \rightleftharpoons Ni(OH)_3^- \tag{50}$$

$$Ni^{2+} + 4OH^- \rightleftharpoons Ni(OH)_4^{2-} \tag{51}$$

with

$$\beta_1 = \frac{[NiOH^+]}{[Ni^{2+}][OH^-]} \tag{52}$$

$$\beta_2 = \frac{[Ni(OH)_2^\circ]}{[Ni^{2+}][OH^-]^2} \tag{53}$$

$$\beta_3 = \frac{[Ni(OH)_3^-]}{[Ni^{2+}][OH^-]^3} \tag{54}$$

$$\beta_4 = \frac{[Ni(OH)_4^{2-}]}{[Ni^{2+}][OH^-]^4} \tag{55}$$

$$\begin{aligned} [Ni]_{tot} &= [Ni^{2+}] + NiL + \sum_{n=1}^{4} Ni(OH)_n^{2-n} \\ &= [Ni^{2+}] \left(1 + K_{NiL}[L^{2-}] + \sum_{n=1}^{4} \beta_n \cdot [OH^-]^n\right) \end{aligned} \tag{56}$$

The combination of equations (45) and (56) results in:

$$K_s^{Ni} = \frac{\{RCOONi^+\}}{\{RCOO^-\} \cdot [Ni]_{tot} \cdot \gamma_{Ni} / \left(1 + K_{NiL}[L^{2-}] + \sum_{n=1}^{4} \beta_n [OH^-]^n\right)} \tag{57}$$

With $\{RCOONi^+\}/[Ni]_{tot} = R_a^{Ni}$ and $\{RCOO^-\} = CEC$, equation (57) is transformed in:

$$K_s^{Ni} = \frac{R_a^{Ni}}{CEC \cdot \gamma_{Ni} / \left(1 + K_{NiL}[L^{2-}] + \sum_{n=1}^{4} \beta_n [OH^-]^n\right)} \tag{58}$$

or

$$R_a^{Ni} = \frac{K_s^{Ni} \cdot CEC \cdot \gamma_{Ni}}{1 + K_{NiL}[L^{2-}] + \sum_{n=1}^{4} \beta_n [OH^-]^n} \tag{59}$$

$$R_a^{Ni} = \frac{K_s^{Ni} \cdot \alpha \cdot CEC_{max} \cdot \gamma_{Ni}}{\left(1 + K_{NiL}[L^{2-}] + \sum_{n=1}^{4} \beta_n [OH^-]^n\right)} \tag{60}$$

R_a^{Ni}	=	concentration ratio of Ni (cm)
K_s^{Ni}	=	surface complexation constant ($cm^3/\mu eq$)
K_{NiL}	=	stability constant of the NiL complex (M^{-1})
β_n	=	hydrolysis constant of $Ni(OH)_n^{-2+n}$
$[L^{2-}]$	=	concentration of ligand L in solution (M)
$[OH^-]$	=	concentration of OH^- in solution (M)

Equation (60) forms the basic equation describing the adsorption of Ni^{2+} on bitumen as a function of pH and concentration of competing ligands L in solution. $K_{NiL} \cdot [L^{2-}]$ in equation (60) equals 0 in this case, since no organic or inorganic ligands other than OH^- were present.

The solid line in Fig. 6.1 displays the least square fit of the R_a^{Ni} calculated by equation (60). The value of the K_s^{Ni} derived from the least square fit equals 856 ± 122. The other parameters used were fixed and are summarized in Table 6.1. The hydrolysis constants of Ni^{2+} were taken from Baeyens and McKinley [3]. The theoretical curve describes the evolution of the R_a^{Ni} as a function of pH. An increase of R_a^{Ni} in the pH range 7-9 is noticed, a maximum at pH 9.2 and a decrease in R_a^{Ni} at pH > 9.2. At pH values >11, the adsorption of Ni^{2+} is completely absent.
Figure 6.2 shows the adsorption of $^{63}Ni^{2+}$ (R_a^{Ni}) as function of the Na^+ concentration in the liquid phase at a constant pH value of 8.3. The higher the Na^+ concentration, the higher the adsorption of Ni^{2+}. According to the Ionizable Surface Group model, the deprotonation of the surface carboxyl groups depends strongly on the ionic strength of the liquid phase between pH 6 and 11. The adsorption capacity (CEC) thus increases with increasing ionic strength.

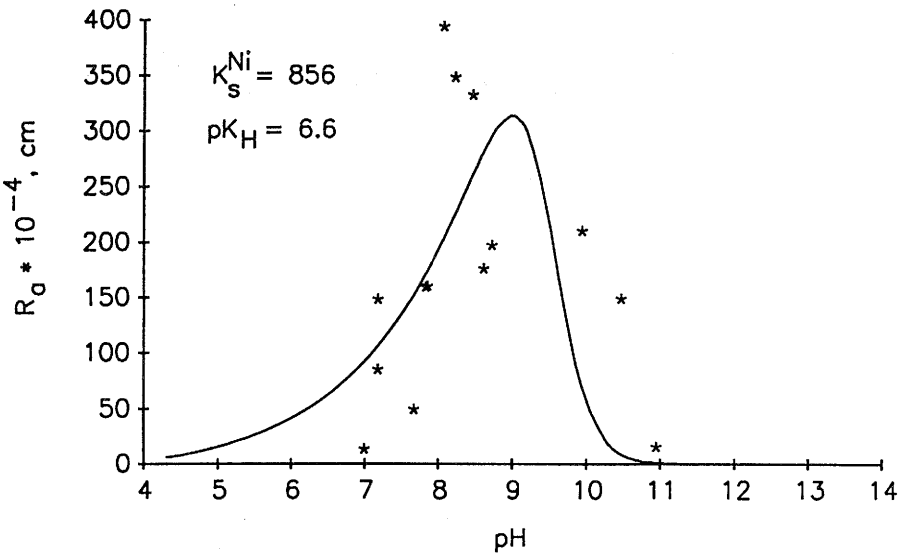

Figure 6.1: Adsorption of Ni^{2+} on bitumen as a function of pH.

Table 6.1: Parameter values used in equation (60) to describe the adsorption of Ni^{2+} on bitumen

Parameter	Value
pK_H	6.6
K_s^{Ni}	856
CEC_{max}	2.28
β_1	$10^{4.27}$
β_2	$10^{8.0}$
β_3	10^{12}
β_4	10^{12}

When the ionic strength is raised from 0.001 M to 0.01 M at pH 8.3, alpha increases from 0.15 to 0.29. The CEC (CEC = $CEC_{max} \cdot \alpha$) thus increases by a factor of 2 from 0.34 to 0.66 μeq/m^2. Consequently, the distribution ratio increases by a factor of two by raising the ionic strength from 0.001 M to 0.01 M at this pH. The solid line in Figure 6.2 is a least square fit of the experimental data by equation 60. The value of K_s^{Ni} derived from this plot equals 702 $\pm$ 35 and is very similar to the value (856) derived earlier. The experimental data can be reasonably well described by equation (60). From this data, it seems that the adsorption reaction (surface complexation) is independent on the ionic strength. Consequently, the surface complexation can be considered as an inner sphere surface complexation reaction. The adsorption (R_a^{Ni}), however, depends on the ionic strength.

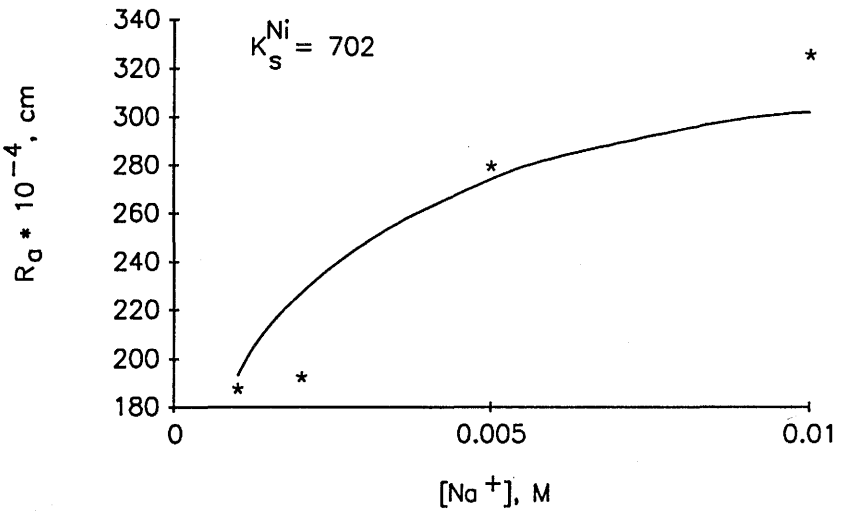

Figure 6.2: Adsorption of Ni^{2+} on bitumen as a function of the Na^+ concentration at pH = 8.3

6.3 Adsorption of Ni^{2+} on bitumen under near field conditions

Equation (60) allows us to evaluate the adsorption of Ni^{2+} on bitumen under near field conditions (cementitious environment). At these high pH values, Ni^{2+} is completely hydrolysed ($Ni(OH)_3^-$: 72%; $Ni(OH)_4^{2-}$: 28%) [3,30]) and adsorption on bitumen is completely negligible. The R_a^{Ni} values can be estimated to be $<10^{-6}$ cm.

7 Evaluation of the adsorption of radionuclides on bitumen

7.1 The adsorption of uranium and americium

Equation (60) can be used to evaluate the adsorption of other cationic radionuclides on bitumen. Let us consider the adsorption of uranium and americium under oxic conditions. Under these conditions, U(VI) and Am(III) are predominant. As no information is available on the surface complexation constants K_s^{Am} and $K_s^{UO_2}$ on bitumen, reasonable estimations have to be made.

To facilitate this estimation exercise, comparison with stability constants of metal–acetate complexes in solution were made. Table 7.1 gives an overview of stability constants of a few 1:1 metal–acetate complexes.

Table 7.1: Stability constants of complexes between M and acetate [23]

Metal	log K_1	K_1
Sr^{2+}	1.19 (I=0, 25°C)	15.5
Ni^{2+}	1.43 (I=0, 25°C)	26.2
Am^{3+}	2.78 (I=0, 20°C)	602
UO_2^{2+}	3.03 (I=0, 20°C)	1071

The stability constant of Ni^{2+} is about 2 times higher than the one for Sr^{2+}. The Am^{3+} and UO_2^{2+} constants are 23 and 41 times higher than the Ni^{2+} constants. Taking the surface complexation constant for Ni^{2+} as a reference and assuming a constant ratio between surface COOH and solution acetate constants, one can calculate surface complexation constants of 20000 (Am^{3+}) and 35000(UO_2^{2+}) as reasonable estimates. Comparison with interaction constants on humic acids is less appropriate since in this case both OH and COOH groups are involved in the complexation reaction.
Figure 7.1 displays the evolution of R_a for UO_2^{2+} and Am^{3+} as a function of pH. The values of K_s^{Am} and $K_s^{UO_2}$ were varied, for illustration, between 1000 and 40000. The values of the other parameters used for the calculations are given in Table 7.2. It is assumed that only the hydrated cation adsorbs on the bitumen surface. This is probably an oversimplification of the adsorption process but, nevertheless, enables one to make realistic estimations of the extend of adsorption on the bitumen surface.

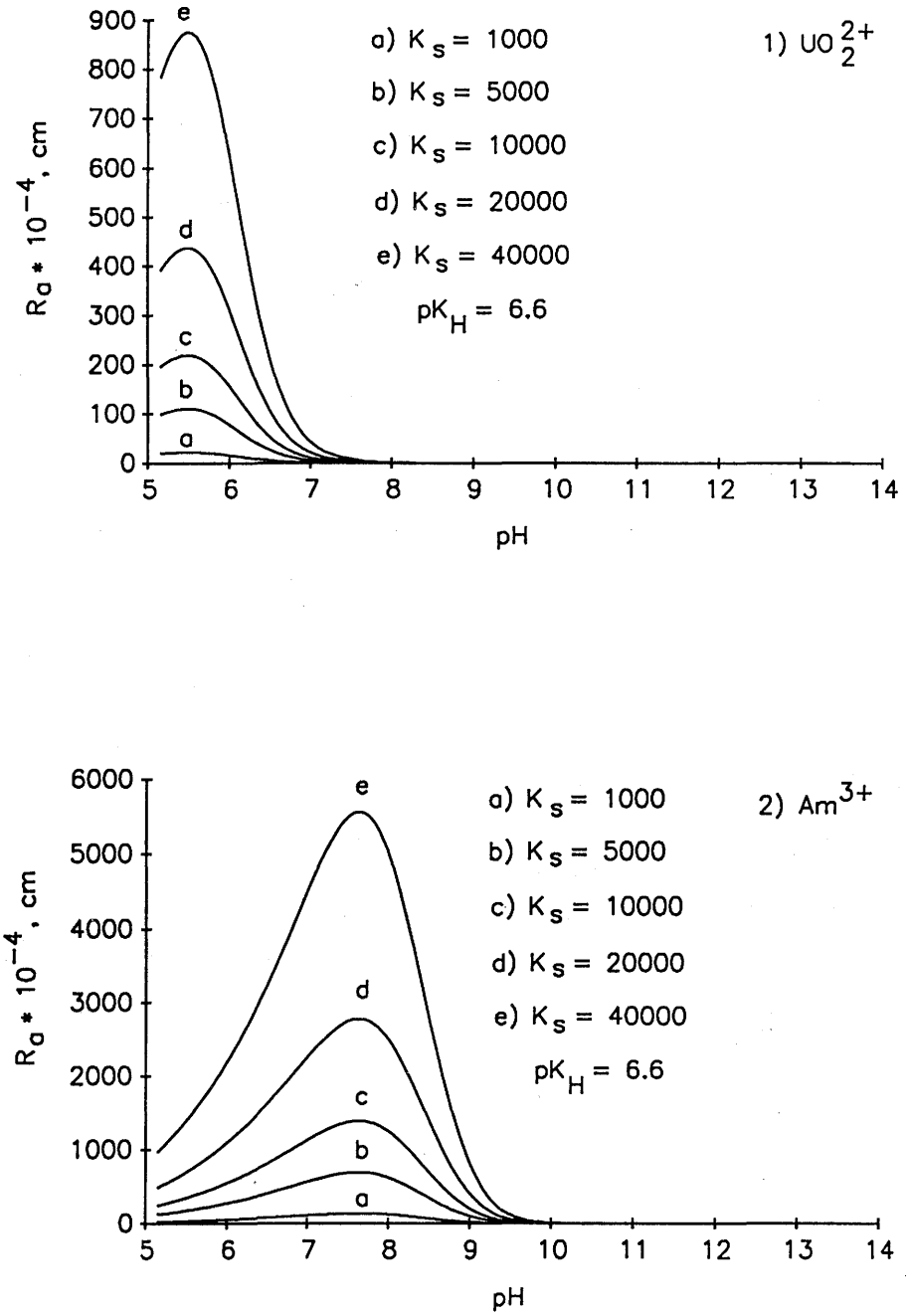

Figure 7.1: Adsorption of UO_2^{2+} (1) and Am^{3+} (2) on bitumen as a function of pH as calculated from equation (60)

Table 7.2: Parameter values used in equation (60) to calculate adsorption of Am^{3+} and UO_2^{2+} on bitumen [17]

Parameter	Value	Species
pK_H	6.6	–
CEC_{max}	2.28	–
$\log \beta_1$	6.0	$Am(OH)^{2+}$
$\log \beta_2$	11.10	$Am(OH)^{+}$
$\log \beta_3$	15.50	$Am(OH)_3^o$
$\log \beta_4$	18.90	$Am(OH)_4^-$
$\log \beta_1$	8.20	$UO_2(OH)^{+}$
$\log \beta_2$	16.0	$UO_2(OH)_2^o$
$\log \beta_3$	18.4	$UO_2(OH)_3^-$
$\log \beta_4$	18.20	$UO_2(OH)_3^{2-}$

The same observations can be made as for Ni^{2+}. The adsorption (R_a) increases as a function of pH, reaches a maximum and decreases again at higher pH values. The pH at which a maximum occurs depends on the values of the hydrolysis constants. The hydrolysis constants have a relative large uncertainty. This, however, has no influence on the conclusions that can be drawn from the calculations. At pH values typical of a cementitious environment, adsorption of both Am^{3+} and UO_2^{2+} is expected to be negligible due to a complete hydrolysis.

For cationic, hydrolyzable radionuclides present in the waste matrix, one can conclude, in general, that no or very weak adsorption on bitumen has to be expected in a cementitious environment.

7.2 Adsorption of anionic radionuclides on bitumen

Anionic radionuclides such as $^{36}Cl^-$, $^{125}I^-$, $^{99}TcO_4^-$, $^{14}CO_3^{2-}$ are not expected to adsorb on the negatively charged bitumen surface.

8 Conclusions

Bitumen has a negatively charged surface due to the deprotonation of weakly acid carboxyl groups present on its surface. The surface charge, and consequently also the adsorption capacity, depends on the pH of the bulk solution in contact with the surface. The electric properties of the bitumen can be described well by the "Ionizable Surface Group" model.

The density of surface carboxyl groups was determined by $Co(NH_3)_6^{3+}$ and equals 2.3 μeq/m^2 or $1.37 \cdot 10^{18}$ groups/m^2.

Cs^+, Sr^{2+} and Ni^{2+} adsorb on the bitumen surface according to three different processes, i.e. ion exchange, outer sphere complexation and inner sphere complexation respectively. The affinity for the surface increases in the order $Cs^+ < Sr^{2+} < Ni^{2+}$.
In a cementitious environment, Cs^+ and Sr^{2+} adsorption on bitumen is negligible due to competition with Na^+, K^+ and Ca^{2+} present in the cement pore water in contact with the bitumen surface.
The adsorption of Ni^{2+} on bitumen is also negligible because the formation of neutral and anionic hydroxo complexes in solution competes very strongly with the adsorption reactions. Other hydrolysable radionuclides (Am^{3+}, UO_2^{2+}) are expected to behave similarly to Ni^{2+}.

Anionic radionuclides are not expected to adsorb on the negatively charged bitumen surface.

It can be generally concluded that the expected R_a values, for radionuclides on bitumen in a cementitious environment, range from 10^{-4} to $< 10^{-6}$ cm. An effect of bitumen on retardation of radionuclides should not be expected and consequently, it is recommended that the adsorption of radionuclides on bitumen is ignored in the safety assessment studies.

9 Acknowledgement

The authors like to thank R. Keil for the chemical analysis and M. Mohos for the electron micrographs.
Thanks also to Dr. A. Maes (KU Leuven, Belgium), Dr. B. Baeyens, Prof. R. Grauer and Dr. I. McKinley (NAGRA) for their comments on the manuscript.
This work was supported financially by the Swiss National Cooperative for the Storage of Radioactive Wastes, NAGRA.

10 References

[1] Alaluusua M., Hakanen M., 1987
Sorption of Cesium, Strontium, Cobalt and Technetium in mixtures of concrete, crushed rock and bitumen
Report YJT-87-10, 1987, Helsinki, Finland.

[2] Anderson K., 1983
Transport of radionuclides in Water/Mineral systems
Ph.D. Thesis, ISBN 91-7032-105-1, Chalmers University, Goteborg.

[3] Baeyens B. and McKinley I.G., 1989
A PHREEQE Database for Pd, Ni and Se
PSI report no. 34, Würenlingen and Villigen, Switzerland
Nagra NTB 88-28, Baden, Switzerland.

[4] Buffle J., 1988
Complexation Reactions in Aquatic Systems: an Analytical Approach.
Ellis Horwood Limited, p. 692.

[5] Burnay S.G., 1987
Sorption effects in the leaching of ^{137}Cs from organic matrix waste forms
AERE R 12421 DOE/RW/87.083, August 1987.

[6] Chow R.S. and Takamura K., 1988
Electrophoretic Mobilities of Bitumen and Conventional Crude-in-Water Emulsions Using the Laser Doppler Apparatus in the Presence of Multivalent Cations
Journal of Colloid and Interface Science 125, 212-225.

[7] Chow R.S. and Takamura K., 1988
Effects of Surface Roughness (Hairiness) of Latex Particles on Their Electrokinetic Potentials
Journal of Colloid and Interface Science 125, 226-236.

[8] Dalang F., 1977
Zur Adsorption von Kationen an die Metalloxid-Wasser-Grenzfläche. Die Adsorption von robusten Kobaltkomplexen
Ph.D. Thesis, Diss. Nr. 5916, ETH Zürich, Switzerland.

[9] Danielli J.F., 1937
The Relations between Surface pH, Ion Concentrations and Interfacial Tension
Proc. Roy. Soc. London, Ser B, 122, 155-174.

[10] Diamond R.M. and Whitney D.C., 1966
Resin selectivity in dilute to concentrated aqueous solutions
in : "Ion exchange" Volume I, Ed. J.A. Marinsky
Marcel Dekker, In., New York, p. 277-351

[11] Eisenman G., 1962
Biophys. J. Suppl. 2, 259-323

[12] Eldridge R.J. and Treloar F.E., 1970
Binding of counterions to polyacrylate solutions
J. Phys. Chem. 74, 1446-1449

[13] Eschrich H., 1980
Properties and long term behaviour of bitumen and radioactive waste–bitumen mixtures
KBS–TR–80–14, KBS, Stockholm, Sweden.

[14] Hietanen R., Alaluusua M., Jaakkola T., 1985
Sorption of Cesium, Strontium, Iodine, Nickel and Carbon in mixtures of concrete, crushed rock and bitumen
Report YJT-85-38, 1985, Helsinki, Finland.

[15] IUPAC 1975
"Ion Exchange Equilibrium Constants", compiled by Y. Marcus and D.G. Howery
Butterwords, London.

[16] Maes A., van Elewijck F., Vancluysen J., Tits J. and Cremers A., 1989
Cobaltihexammine as an index cation for measuring the cation exchange capacity of humic acids
Proceedings of the International Symposium on Humic Substances in the Aquatic and Terrestrial Environment, Linkoping, Sweden, August 21-23, 1989. In Press in Lecture Notes in Earth Sciences.

[17] MINEQL/PSI database.

[18] Morel R., 1975
Etudes expérimentales des phénomènes d' échange sur différentes minéraux argileux
Annales Agronomiques 6, 5-90

[19] Neumann H.J. et al., 1981
Bitumen und seine Anwendungen: Bitumen, Asphalt, Industriebitumen
Kontakt & Studium, Band 63. Expert Verlag 7031 Grafenau 1/Württ.

[20] Novozamsky I., Beek J., Bolt G.A., 1978
Chemical Equilibria
In : "Soil Chemistry. A. Basic elements." Ed. G. Bolt and M. Bruggenwert
Elsevier Scientific Publishing Company. Amsterdam–Oxford–New York. p 13–42.

[21] Perdue E.M., Reuter J.H., Parrish R.S., 1984
A Statistical Model of Proton Binding by Humus
Geochim. Cosmochim. Acta 48, 1257.

[22] Reichenberg D., 1966
Ion Exchange Selectivity
In: "Ion exchange" Volume 1, Ed. J.A. Marinsky
Marcel Dekker, In., New York, p. 227-276.

[23] Sillen L.G. and Martell A.C., 1971
Stability constants of metal-ion complexes
Special Publication 25, Chemical Society, Burlington House, W1 London.

[24] Stone-Masui J. and Watillon A., 1975
Characterization of Surface Charge on Polystyrene Latices
Journal of Colloid and Interface Science 52, 479-503.

[25] Takamura K., 1985
Physico–chemical characterization of Athabasca oil sand and its significance to bitumen recovery
AOSTRA Journal of Research 2, 1-10

[26] Takamura K. and Chow R.S., 1985
The Electric Properties of the Bitumen/Water Interface
Part II: Application of the Ionizable Surface-Group Model
Colloids and Surfaces 15, 35-48.

[27] Takamura K. and Wallace D., 1987
Experimental and theoretical studies of the hot water processability of different grades of Athabasca oil sand
In : "Flocculation in Biotechnology and Separation Systems", ed. Yosry A. Attia, Process Technology Proceedings 4, Elsevier Science Publishers B.V., Amsterdam, 579-598

[28] Takamura K. and Wallace D., 1988
The physical chemistry of the hot water process
The Journal of Canadian Petroleum Technology 27, 98-106

[29] Tits J., 1990
Characterization of soil humic substances : relevance for zinc speciation in soils.
Ph.D. Thesis, Dissertationes de Agricultura Nr.196, Faculty of Agronomy, Catholic University of Louvain, Belgium.

[30] Van Loon L.R. and Kopajtic Z., 1990
Complexation of Cu^{2+}, Ni^{2+} and UO_2^{2+} by radiolytic degradation products of bitumen
PSI-report no. 66, Würenlingen and Villigen, Switzerland.
Nagra NTB 90-18, Baden, Switzerland.